THESIS FOR THE DEGREE OF DOCTOR OF PHILOSOPHY

Imaging mass spectrometry for *in situ* lipidomics: from cell structures to cardiac tissue

Sanna Sämfors

Department of Chemistry and Chemical Engineering

Chalmers University of Technology

Gothenburg, Sweden

2018

Imaging mass spectrometry for *in situ* lipidomics: from cell structures to cardiac tissue
Sanna Sämfors

ISBN: 978-91-7597-729-4

Doktorsavhandlning vid Chalmers tekniska högskola
Ny serie nr 4410
ISSN: 0346-718X

Department of Chemistry and Chemical Engineering
Chalmers University of Technology
SE–412 96 Gothenburg
Sweden
Telephone + 46 (0) 31 – 772 1000

Cover: Illustration by the author showing a drawing of a heart and brain cells.

Typeset by the author using LaTeX.

Printed by Chalmers Reproservice
Göteborg, Sweden 2018

Imaging mass spectrometry for *in situ* lipidomics: from cell structures to cardiac tissue

SANNA SÄMFORS

Department of Chemistry and Chemical Engineering

Chalmers University of Technology, Gothenburg, Sweden, 2018

Abstract

Imaging of cells and tissues is important for studying different processes within biological systems due to the spatial information provided for different molecular species during imaging. One powerful imaging technique is mass spectrometry imaging (MSI). It is a label free technique that provides chemical information of a sample at the same time as it allows for imaging at high spatial resolution. Time-of-flight secondary ion mass spectrometry (ToF-SIMS) uses a focused primary ion beam to ablate and ionise molecules from the top layers of the sample surface which makes it a very surface sensitive technique. Recent developments in high energy gas cluster ion beam (GCIB) technology for ToF-SIMS has greatly improved the imaging of higher mass species, such as intact lipids. Lipids are important molecules found in all living organisms. They are used as building blocks for cells and are involved in a variety of important cellular processes such as energy storage and acting as important mediators in many signalling pathways, making them an interesting target for imaging studies. In this thesis, the ToF-SIMS imaging technique has been applied to both tissues and cells in order to perform *in situ* lipidomics analysis of various samples. Development of sample treatment methods that provides easier data interpretation and other method development for improving secondary ion yields have also been implemented in this work. In paper I, enhancement of negative secondary ion yields was induced by a combination of ion bombardment using a GCIB with simultaneous caesium flooding, for both inorganic and organic substrates. In paper II, ToF-SIMS imaging with a GCIB was used together with LC-MS to elucidate changes in lipid composition 6 hours after an induced myocardial infarction in mouse heart. The spatial information from the MSI allowed correlation of specific lipid species to infarcted and non-infarcted regions of the heart. Localised lipid accumulation was discovered in specific regions of the heart. In paper IV, these lipid changes were tracked over longer periods of time, 24 hours and 48 hours after infarction, and progression of the infarcted area was observed. In paper III, a simple method was developed in order to aid interpretation of the complex mass spectra collected from ToF-SIMS experiments of complex tissue sample such as heart tissue. Salt adduct formation was demonstrated as a means to discriminate between diacylglyceride and triacylglyceride, which are usually impossible to distinguish during ToF-SIMS analysis. In paper V, lipid changes in PC12 cell membranes were analysed after incubation with the essential fatty acids, omega-3 and omega-6. Using deuterium labelled fatty acids made it possible to track incorporation into phospholipids as well as the relative amount of each.

Keywords: *Mass spectrometry imaging, ToF-SIMS, Lipidomics, Myocardial infarction, PC12 cells, Sample preparation, Gas cluster ion beam, Cell membrane*

List of Publications

The following publications constitute the basis for this thesis:

Paper I **Significant enhancement of negative secondary ion yields by cluster ion bombardment combined with cesium flooding**, Patrick Philipp, Tina B. Angerer, Sanna Sämfors, Paul Blenkinsopp, John S. Fletcher and Tom Wirtz, *Analytical Chemistry*, 2015, 87(19), pp 10025-10032.

Paper II **Localised lipid accumulation detected in infarcted mouse heart tissue using ToF-SIMS**, Sanna Sämfors, Marcus Ståhlman, Martina Klevstig, Jan Borén, John S. Fletcher, *International Journal of Mass Spectrometry*, 2017, https://doi.org/10.1016/j.ijms.2017.09.012.

Paper III **Salt adduct formation for the discrimination of diacylglyceride and triacylglyceride ions in ToF-SIMS analysis**, Sanna Sämfors, Andrew G. Ewing, John S. Fletcher, *Rapid Communications in Mass Spectrometry*, *Submitted*.

Paper IV **Spatio-temporal changes in lipid composition in infarcted mouse heart tissue elucidated by ToF-SIMS imaging**, Sanna Sämfors, Jan Borén, John S. Fletcher, *Manuscript in preparation*.

Paper V **Relative quantification of deuterated omega-3 and -6 fatty acids and their lipid turnover in PC12 cell membranes using ToF-SIMS**, Mai Hoang Philipsen, Sanna Sämfors, Per Malmberg, Andrew G. Ewing, *Analytical Chemistry, Submitted*.

Contribution Report

Paper I I performed sample preparation of cell samples and performed the data analysis and interpretation of these samples.

Paper II Planned and designed the project together with the co-authors. Performed the mass spectrometry imaging experiments, did the data analysis and interpretation, made the graphs and figures and was the main author of the manuscript. Handled the journal submission process and review together with John Fletcher.

Paper III Planned and designed the project together with the co-authors. Performed the experiments, did the data analysis and interpretation, made the graphs and figures and was the main author of the manuscript. Handled the journal submission process.

Paper IV Planned and designed the project together with the co-authors. Performed the mass spectrometry imaging experiments, did the data analysis and interpretation, made the graphs and figures and was the main author of the manuscript.

Paper V Performed the J105 mass spectrometry analysis. Took part in analysing and interpreting the data. Wrote the manuscript together with Mai Hoang Philipsen.

Contents

List of Abbreviations

ATP	Adenosine triphosphate
CAR	Acylcarnitine
CAT	Carnitine-acylcarnitine translocase
CE	Cholesterol ester
CER	Ceramide
CL	Cardiolipin
CoA	Coenzyme A
CPT1	Carnitine palmitoyltransferase I
CPT2	Carnitine palmitoyltransferase II
CT	Computed tomography
DAG	Diglyceride
ESI	Electrospray ionisation
FA	Fatty acid
GCIB	Gas cluster ion beam
IP_3	Inositol triphosphate
LC-MS	Liquid chromatography mass spectrometry
LMIG	Liquid metal ion gun
LPI	Laser post ionisation
MAF	Maximum autocorrelation factor
MALDI	Matrix assisted laser desorption/ionisation
MI	Myocardial infarction
MRI	Magnetic resonance imaging
MS	Mass spectrometry
MSI	Mass spectrometry imaging
MVA	Multivariate analysis
NGF	Nerve growth factor
PA	Phosphatidic acid
PC	Phosphatidylcholine
PCA	Principal component analysis
PE	Phosphatidylethanolamine
PG	Phosphatidylglycerol

PKC	Protein kinase C
PI	Phosphatidylinositol
PIP	Phosphoinositide
PS	Phosphatidylserine
PUFA	Polyunsaturated fatty acid
SEM	Scanning electron microscopy
SIMS	Secondary ion mass spectrometry
SM	Sphingomyelin
TAG	Triglyceride
TFA	Trifluoroacetic acid
ToF	Time-of-flight
VLDL	Very low density lipoprotein
VLDLr	Very low density lipoprotein receptor

"Remember to look up at the stars and not down at your feet. Try to make sense of what you see and wonder about what makes the universe exist. Be curious. And however difficult life may seem, there is always something you can do and succeed at. It matters that you don't just give up." - ***Stephen Hawkins***

CHAPTER 1

Introduction

Imaging can be a powerful method providing important spatial information of a sample. It is said that ”a picture is worth a thousand words”, and in many cases especially in application areas such as in medical imaging, this is true. The development of many medical imaging techniques including x-ray, mammography, MRI and CT have provided new tools for diagnosis of many diseases. It has also offered insights in understanding the pathology process for certain diseases. Other imaging methods, like fluorescent imaging have given us the ability to look at very small features and biochemical processes occurring within a single cell, providing even better understanding of many disease processes. On the other hand, analytical techniques providing specific chemical information are also very useful for diagnoses and understanding of diseases. One of these is mass spectrometry, an analytical technique that can be used for determining the chemical composition of a sample. It has been applied in various fields e.g. for diagnosis of different diseases where levels of different biomolecules can be measured in tissues or bodily fluids such as blood and urine. The mass spectrometry technique also allows for imaging to be performed. Imaging mass spectrometry combines the advantages that collecting a 2D picture provides with the ability to collect chemical information simultaneously on a wide variety of samples. With this method, chemical maps can be created of the sample, providing a direct link between chemical changes and morphological features within the sample allowing for *in situ* analysis without the need for extraction methods. This can be a very powerful tool for diagnosis and better understanding of disease processes occurring in terms of the actual chemical changes. It also opens the ability to create very precise drugs, that can counteract the chemical changes occurring by affecting very specific targets. One of the advantages that mass spectrometry imaging has over other imaging methods is that it is typically a label free technique which means no prior knowledge of the sample is needed, thus it is useful to apply on samples where the knowledge of the chemical composition is limited.

In this thesis, a specific imaging mass spectrometry technique has been applied, called time-of-flight secondary ion mass spectrometry (ToF-SIMS). In ToF-SIMS, primary ions are used for ejecting material from the sample surface. The advantage

of using ions, is that they are fairly easy to focus down to small spot sizes, making it possible for chemical imaging at high spatial resolution. ToF-SIMS has in many studies been shown to be a good method for lipid analysis [1]. Lipids are a large group of compounds found in all living organisms. They carry out many important functions in biological systems, such as providing structural integrity for cell membranes, function as energy storage molecules and serve as important signalling molecules. Changes in lipid composition in a sample can be an early sign of disease. Lipids have been shown to play roles in disease processes such as cancer [2], heart failure [3] and Alzheimer's disease [4], making them very important targets to study. Applying ToF-SIMS imaging on various tissues for studies of lipid composition in both diseased and healthy tissues can help explain the disease process by providing spatial distributions of a wide variety of lipid species simultaneously.

The aim of this thesis has been to expand the application areas of the ToF-SIMS imaging technique for lipid analysis of biological samples using a novel gas cluster ion beam. To achieve this, a new instrumental set-up has been assessed in terms of enhancement of secondary ion yields as well as the application of new sample preparation methods for easier interpretation of spectra of complex biological tissues. Also, heart tissue has been imaged following a heart attack, in order to determine lipid changes occurring during and after the heart attack. The tissue has been analysed at different time points to track lipid changes temporally, where the goal has been to gain a better understanding of the breakdown and repair of heart tissue following a heart attack. Finally, ToF-SIMS analysis has been applied to cells, where incorporation of omega-3 and omega-6 fatty acids into the cell membrane of the neuron-like PC12 cells has been tracked. The goal has been to better understand the effects of essential fatty acids on cell membrane composition in order to assess their beneficial effects. The main goal for the investigations included in the thesis has been to advance the ToF-SIMS imaging technique for biological applications. The outline of the thesis is as follows: Lipid structures and their biological function are introduced in Chapter 2. The mass spectrometry technique, including ToF-SIMS and ToF-SIMS imaging, is described in detail in Chapter 3. In Chapter 4, the methodologies applied in the studies included in this thesis are described. The work leading to scientific publications is summarised in Chapter 5 and concluded in Chapter 6.

CHAPTER 2

Lipids in biological systems

Lipids are important biological compounds and serve many purposes in living organisms, where the main functions are as structural components in cell membranes, energy storage and as signalling molecules. Lipids are defined as a class of naturally occurring organic compounds that are insoluble in water but soluble in non-polar organic solvents. They include compounds such as natural oils, waxes, steroids, fat-soluble vitamins, mono- di- and triglycerides, phospholipids, and others. There is great structural variety among lipids but many lipid structures are amphiphilic, meaning that they have both a hydrophobic and a hydrophilic part. Their amphiphilic nature allows them to form structures such as membranes in an aqueous environment, making them useful building blocks for cells. This chapter covers the major lipid classes and their structures that are found in biological systems. It also covers lipid function in the two biological systems studied in this thesis, the cell and heart tissue.

2.1 Lipid classes and structure

Classification of lipids can be difficult since they are structurally very different compounds. A common feature of lipids, though, is that they consist of hydrocarbon chains in different conformations and it is the structure of these that determines their properties and also define classification. According to LIPID MAPS®, an online database for lipidomics research, lipids can be divided into eight categories: fatty acids, glycerolipids, glycerophospholipids, sphingolipids, saccharolipids, polyketides, sterol lipids and prenol lipids [5]. Not all of these classes are covered in this thesis. The next section describes the structure and function of the most common lipid classes found in biological systems, with a focus on mammalian systems.

2.1.1 Fatty acids

Fatty acids (FA) are molecules with a long hydrocarbon chain attached to a carboxylic acid moiety in one end (Figure 2.1). The hydrocarbon chain can be either

saturated, containing no carbon-to-carbon double bonds, or unsaturated, containing one or more double bonds. Most naturally occurring fatty acids consist of an unbranched chain of an even number of carbon atoms. In biological systems, fatty acids exist in the form of either free fatty acids or as esterified fatty acids in phospholipids or other lipids. The function of fatty acids in biological systems is to serve as components of membrane lipids or energy storage in the form of triglycerides, and they also function as precursors for the syntheses of bioactive lipids.

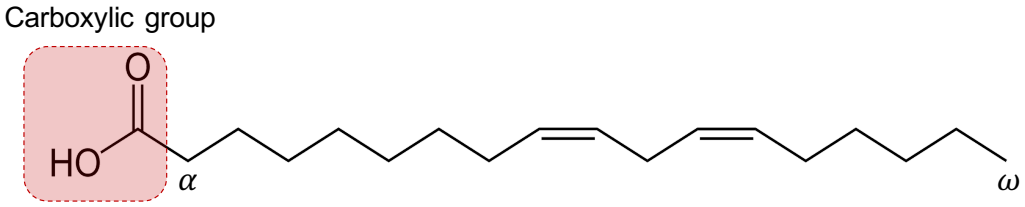

Figure 2.1. Structure of the fatty acid linoleic acid or FA(18:2). The carbons in the hydrocarbon chain are named by using greek letters where the α is the carbon closest to carboxyl group and the ω is the carbon furthest from the carboxyl group.

The majority of the fatty acids are acquired in the diet but most fatty acids can also be supplied *via* lipid biosynthesis. However, there are two unsaturated fatty acids that cannot be synthesis from precursors in the body and must therefore be acquired by diet. These are called essential fatty acids, and for humans and other animals, there are two polyunsaturated fatty acids (PUFAs) that cannot be synthesised. These are the linoleic (omega-3) acid and the α-linoleic (omega-6) acid, with two and three double bonds, respectively.

The most common fatty acids have trivial names, such as linoleic acid and palmitoleic acid, referring to the fatty acids with an 18-carbon chain with two double bonds and a 16-carbon chain with one double bond, respectively. More systematic names, include the number of carbons, double bonds and which configuration the double bonds have (cis (Z) or trans (E)). Also, the systematic name usually includes the position of the double bond in relation to the α (carbon closest to carboxyl group) or the ω (furthest from the carboxyl group) carbon (Figure 2.1). When fatty acids are esterified into glycerolipids or glycerophospholipids, the position of the fatty acids on the glycerol backbone can also be indicated in the name, by sn-1, sn-2 or sn-3 when the fatty acid is attached to the first, second or third

carbon in the glycerol, respectively (Figure 2.2). However, during standard mass spectrometry analysis, the position and configuration of the double bond cannot be identified, leaving the relevant information acquired from the analysis to be the number of carbons and double bonds. Hence, in this thesis, the name of fatty acids are given as: FA(x:y), where the letter x indicates the number of carbons in the fatty acid chain and the letter y indicates the number of double bonds. For esterified fatty acids the name is given as: PC(x:y), where the first two letters indicate the headgroup (in this case PC for phosphocholine headgroup) and the letter x is the number of carbons in the fatty acid chains combined and y indicates the combined number of double bonds.

2.1.2 Glycerolipids

Glycerolipids consist of a glycerol molecule and at least one fatty acid chain linked to the glycerol backbone with an ester bond (Figure 2.2). They are naturally uncharged and apolar molecules. They play a key role, both structurally and functionally, in bacterial, plant and animal membranes. The main glycerolipid found in animals is the triglyceride; however, diglyceride and monoglycerides can also be found but in smaller amount and mainly serve as intermediates or as signalling molecules [6, 7].

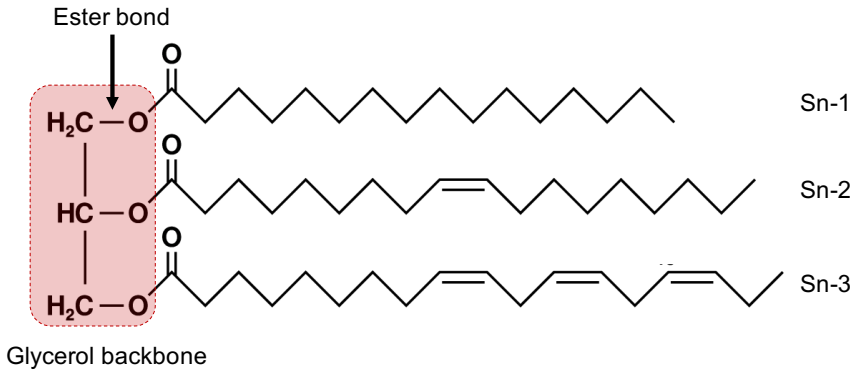

Figure 2.2. Structure of a glycerolipid consisting of a glyceride backbone linked by ester bonds to three fatty acid chains. Sn-1, sn-2 and sn-3 indicates to which carbon on the glycerol backbone the fatty acids are attached to.

Diglyceride

A diglyceride (or diacylglyceride) abbreviated DAG, is a glycerolipid with two fatty acid chains covalently attached to the glycerol backbone. DAGs are involved in a variety of metabolic pathways in biological systems. They are used as building blocks for glycerophospholipids and as components of cellular membranes. Under equilibrium conditions, cell membranes contain a low amount of DAGs, usually ranging between 1-8 mole% [8]. They can, however, localise in specific domains, thus altering the physical properties of the membrane. Due to their molecular shape, with a small polar headgroup and a large non-polar chain domain, they have a large negative spontaneous curvature and therefore changes the cell membrane properties in areas where they are accumulated [9]. DAGs are very important secondary messengers in mammalian cells, and they are a part of a variety of different signalling pathways such as the protein kinase C (PKC) signalling pathway [10, 11]. DAGs can be derived through either hydrolysis of glycerophospholipids *via* specific enzymes that cleave the intact lipids or from *de novo* synthesis [12]. Changes in DAG metabolism have been associated with various diseases such as diabetes [13], cancer [14], and coronary heart disease [15].

Triglyceride

A triglyceride (or triacylglyceride) abbriviated TAG, is a glycerolipid with three fatty acid chains attached to the glycerol backbone. The main function of TAGs is to serve as energy storage for the cell. TAGs are stored in the center of lipid droplets (lipoproteins) surrounded by a monolayer of glycerophopsholipids and hydrophobic proteins [16] and are used for energy storage or as a source of DAGs [17]. Many cell types and organs are able to synthesize TAGs but in animals it is the liver, intestines, and adipose tissue where most of them synthesised and most TAGs are stored in adipose tissue.

2.1.3 Glycerophospholipids

Glycerophospholipids (or more commonly referred to as phospholipids), are major components of the cellular membrane, and are also involved in metabolism and signalling. They have an amphiphilic nature and most commonly consist of two non-polar fatty acid chains and a polar moiety consisting of a phosphate group with a headgroup substituent, all attached to a glycerol backbone by ester bonds (Figure 2.3). The glycerophospholipids can be divided into subclasses depending on which

headgroup substituent is attached to the phosphate group in the sn-3 position of the glycerol backbone . The properties and main function of the phospholipids appears to be determined by which headgroup is attached as well as the degree of saturation of the fatty acids attached.

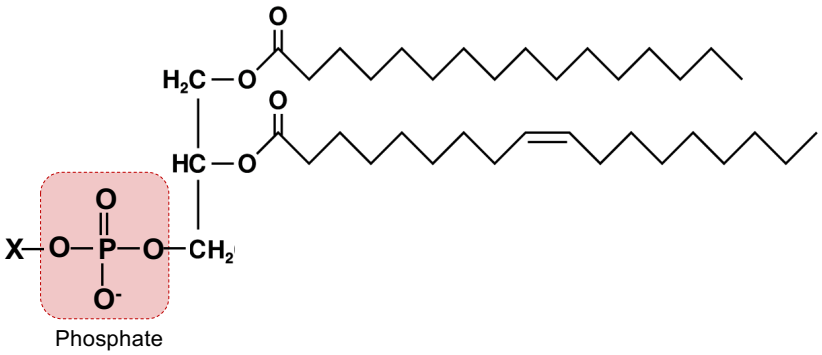

Figure 2.3. General structure of a glycerophospholipid. Two fatty acid chains are attached to a glycerol backbone, and a polar headgroup consisting of a phosphate group with a different headgroup substituent, x, depending on which subclass it is.

Phosphatidic acid

Phosphatidic acid (PA) is the most simple glycerophospholipid with a hydrogen atom as the headgroup substituent attached to the phosphate. This makes it a small and highly charged headgroup. Due to the small headgroup compared to the fatty acid tails, PA is a high curvature lipid with a conical shape and when accumulated it can affect the curvature of the cellular membrane. Therefore, PA is thought to be involved in vesicle formation or other events where high curvature membrane formation is needed. PA is a precursor for the biosynthesis of many other lipids. PA gets converted into DAGs that are further synthesised to a variety of phopholipids, such as phosphatidylinositol, phosphatidylglycerol, phosphatidylserine, phosphatidylcholine and phosphatidylethanolamine. PA is short lived and maintained at low levels in the cell [18] and is readily converted into DAGs. PA also has an important role as a lipid mediator in cell signalling [19] and has been shown to be involved in signalling pathways in proliferation [20], cytoskeletal rearrangement [21], and vesicle trafficking and fusion [22].

Phosphatidylglycerol

Phosphatidylglycerol (PG) is a phospholipid with a glycerol as the headgroup substituent. PG is one of the major components of bacterial membranes [23] but can also be found in plant and animal membranes, but at lower abundance [24]. In mammalian cells it is mainly found on the inner membrane of the mithochondria. In humans, PG acts as a lung surfactant and can be used as an indicator for fetal lung maturity when measured in amniotic fluid [25]. PG is a key intermediate in the biosynthesis of a number of lipids [26], especially of cardiolipin which is an important component in mitochondrial membranes [27].

Phosphatidylcholine

Phosphatidylcholine (PC) is a phospholipid that has a choline as the headgroup substituent. Choline is a quaternary amine with a positive charge that together with the phosphate group with a negative charge, makes the phosphatidylcholine lipid zwitterionic (a molecule with both a positive and a negative charge). Due to its structure, with a polar headgroup and non-polar fatty acid tails, PC is a strong bilayer-forming lipid in aqueous environments [28]. It is the most abundant lipid in the cell membrane of mammalian cells, where it is commonly found in the extracellular leaflet due to its cylindrical shape. It is part of cell signalling as it is a major source of secondary messengers such as DAGs, PA, lysoPA and lysoPC through phospholipse A activity [29]. In mammalian cells, the most common PCs have a saturated fatty acid in the sn-1 position and an unsaturated fatty acid in sn-2 position [30].

Phosphatidylethanolamine

Phosphatidylethanolamine (PE) is a phospholipid where the headgroup substituent is an ethanolamine group. These lipids are ubiquitous for all living cells and are the second most abundant phospholipid in mammalian cells, after phosphatidylcholine, where they make up about 15-25% of the total lipids [31]. They are enriched in the inner leaflet of the lipid bilayer and on the inner mitochondrial membrane [32]. Due to the small polar headgroup in contrast to the larger fatty acid tails, PE has a conical shape and is therefore thought to be involved in processes such as membrane fusion and fission events, where high curvature is needed [33]. It is found particularly in nervous tissue such as the white matter of brain, nerves, neural tissue, and in spinal cord, where it makes up 45% of all phospholipids [34]. PE is

mainly synthesised in the endoplasmic reticulum but can also be synthesised in the mitochondria.

Phosphatidylserine

Phosphatidylserine (PS) has a serine as the headgroup substituent. PS is a part of the cell membrane where it plays a key role in cell signalling, especially during apoptosis. Normally, it is heterogeneously distributed in the cell membrane and are actively held on the inner leaflet of the membrane. During apoptosis however, PS can move freely between both leaflets of the membrane and when PS is detected on the extracellular leaflet, it acts as a signal for macrophage activation for removal of apoptotic cells [35, 36]. PS can be synthesised by two different pathways in the cell, where enzymes replace the choline or ethanolamine headgroup on PC and PE lipids, respectively, to create PS [34].

Phosphatidylinositol

Phosphatidylinositol (PI) is a phospholipid with an inositol ring as the headgroup substituent. The phosphate group gives the molecule a negative charge at physiological pH. Phosphatidylinositols make up a minor component of eukaryotic cell membranes and can mainly be found on the cytosolic side. The inositol ring can be reversibly functionalised by phosphorylation at three different places on the ring, creating different phosphoinositides (PIPs). There are seven naturally known phosphoinositde isomers, of which PI(4)P and PI(4,5)P_2 are most abundant in mammalian cells [37]. The PIPs are involved in, and regulate, a large number of cellular events, such as cell signalling, membrane trafficking, cytokinesis, and organelle distinction [38]. They play a major role in lipid-protein interaction, either by direct interaction by binding or by mediating signalling pathways. The direct signalling is achieved by direct binding of the inositide headgroup to cytosolic or membrane proteins which causes activation of signalling pathways. The different PIPs are heterogeneously distributed in the cell membrane. The PIs are synthesised in the endoplasmic reticulum and transported to the membrane by vesicles or transfer proteins that are found in the cytosol [39].

Cardiolipin

Cardiolipin (CL) is a polyglycerophospholipid, meaning that it has a dimeric structure where two phosphatidyl moieties are linked by a central glycerol group (Figure

2.4). This means that the cardiolipins have four fatty acid chains, and therefore exhibit a conical shape. CL is most abundant in heart tissue and it was first discovered here, hence its name. It is mainly found in mitochondrial and bacterial membranes. In healthy cells, CL is mainly located on the inner membrane of mitochondria. Here it plays a vital role in energy metabolism by interacting with specific enzymes and proteins. Direct interaction between proteins and CLs supports the structural integrity of proteins by preventing the denaturing and loss of function [40]. They also play a part in the mithocondrial apoptois signalling process. During hypoxia or other fatal processes, the fatty acid content of cardiolipins changes resulting in translocation to the outer membrane of the mitochondria and signals the onset of apoptosis [41]. Changes in cardiolipin composition are connected to diseases like diabetes [42] and heart failure [43]. Cardiolipins can be synthesised from phosphatidylglycerol in the mitochondria [44].

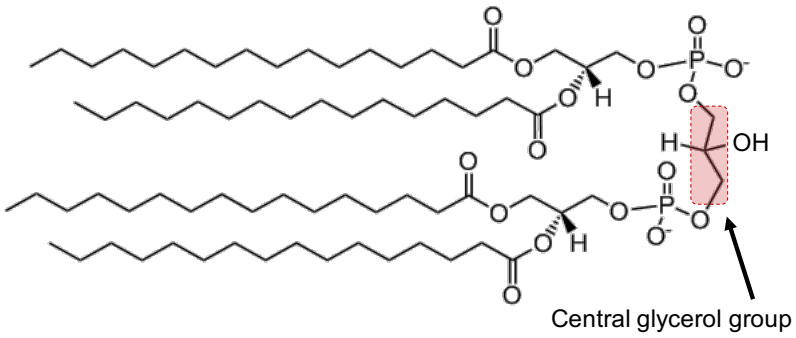

Figure 2.4. General structure of a cardiolipin, with two phosphatidyl moieties linked together by a central glycerol group.

2.1.4 Sphingolipids

Sphingolipids are a class of lipids containing a sphingoside backbone, linked to an acyl group, such as a fatty acid. The backbone is also linked to a headgroup such as phosphoethanolamine, phosphocholine or phosphoserine (Figure 2.5). Sphingolipids are a part of the cell membrane where they help in forming a stable outer leaflet of the plasma membrane in order to protect the cell surface. They are also part of cell recognition and signalling processes. Sphingolipid metabolites are involved in various signalling cascades, acting as important mediators.

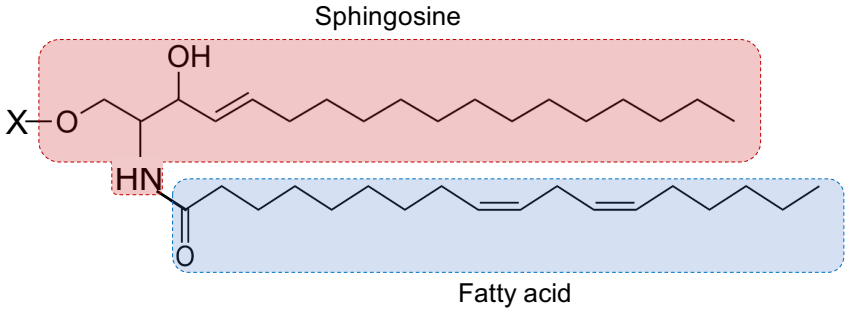

Figure 2.5. General structure of a sphingolipid, with a sphingosine backbone and a fatty acid moiety. The headgroup substituent, x, differs depending on which subclass of sphingolipids.

Sphingomyelin

Sphingomyelin (SM) has either a phsophocholine or a phosphoethanolamine headgroup attached to the sphingosine and fatty acid backbone, where the phosphoethanolamine headgroup is most common in insects and the phosphocholine headgroup in mammalian cells, respectively. They are present in the plasma membrane and are especially prominent in the myelin sheath, a membrane surrounding axons in neurons [45]. Structurally they are similar to PCs as they are cylindrically shaped and zwitterionic with no net charge on the headgroup.

Ceramides

Ceramides (CER) consists of a sphingosine backbone with a fatty acid attached. The headgroup substituent consists of a hydrogen atom. They are found in the cell membrane, where they act as support structures but, more importantly, they participate in a variety of cellular signalling pathways, including regulating differentiation, proliferation and apoptosis [46]. Ceramides are found in high concentrations in skin, where they in combination with cholesterol and saturated fatty acids, create a impermeable protection barrier against micro-organisms [47]. They have also been shown to be important in many pathological processes, such as cancer [48], diabetes [49] and inflammation [50]. In mitochondria, ceramide accumulation is thought to lead to suppression of the electron transport chain which induces production of reactive oxygen species [51] which can initiate apoptotic events. *De novo* synthesis

of ceramide takes place in the endoplasmic reticulum, and they gets transported to the Golgi apparatus by either vesicular trafficking or the ceramide transfer protein. In the Golgi, they can be further metabolised to other sphingolipids, such as sphingomyelins.

2.1.5 Steroids

The steroids are structurally very different from other lipids, but are still classified as lipids due to their insoluble properties in water. Steroids consists of four hydrocarbon rings (Figure 2.6a) with a variety of functional groups that may be attached. The most common steroid in biological systems is cholesterol (Figure 2.6b).

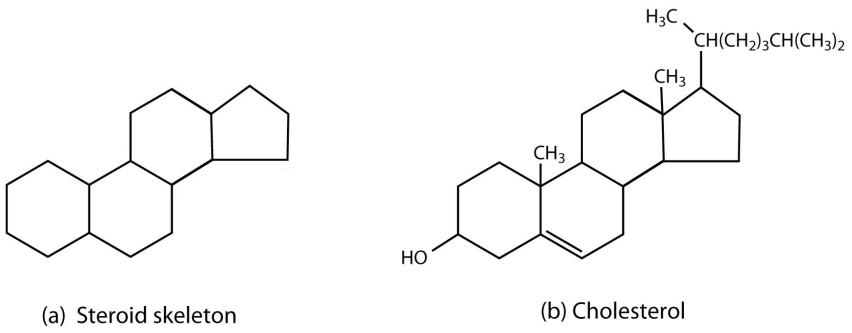

Figure 2.6. Structure of (a) a steroid skeleton and (b) a cholesterol molecule. Image credit: modified from [52].

Cholesterol and cholesterol esters

Cholesterol is a structural component of all mammalian cell membranes and it is essential for maintaining the structure and fluidity of the membrane. Cholesterol intercalates between the phospholipids in the membrane and creates a tighter membrane by binding to the fatty acid chains [53]. Cholesterol in the cell membrane can also change the fluidity properties of the membrane, with more cholesterol creating more rigid membranes [54]. Cholesterol also serves as a precursor for steroid hormones, vitamin D and bile acids [55]. Cholesterol exists as free cholesterol when it is first synthesized in the liver, but is taken up by lipoproteins to allow for transportation in the bloodstream. In the lipoproteins, cholesterol mainly exist in the form of cholesteryl esters (CE). CEs are formed by creation of an ester bond between a cholesterol molecule and a fatty acid [56]. The conversion from cholesterol

to cholesterol esters allows them to be more densely packed into lipoproteins, which greatly increases the transportation capacity of cholesterol in the bloodstream.

2.1.6 Acylcarnitines

Acylcarnitines (CAR) are fatty acyl esters of carnitine. Carnitine and acylcarnitines are essential components of the β-oxidation process described in more detail in chapter 2.2.2. During this process fatty acids are oxidised in order to generate energy. This process takes place on the inner membrane of the mitochondria. To reach the mitochondria, intracellular fatty acids must first undergo esterification with Coenzyme A (CoA) to acyl-CoAs, the activated form of fatty acids. The long chain acyl-CoA can not pass trough the mitochondrial membrane, and needs the assistance of the carnitine transport pathway [57]. An acyl-CoA reacts with a carnitne molecule to form acylcarnitine (Figure 2.7). Acylcarnitines can pass through the mitochondrial membrane, thus delivering the fatty acids needed for the β-oxidation [58]. Carnitine is present in high amounts in heart and skeletal muscle tissue, where acylcarnitines constitute an appreciable amount of the tissue carnitine pool. Both carnitine and acylcarnitine are maintained within narrow limits in the cell by a variety of mechanisms. In fatty-acid oxidation defects, acylcarnitine species accumulate and are released into the circulation system, therefore, acylcarnitne profile analysis in blood, urine and tissues can be used in order to diagnose fatty acid oxidation disorders [59].

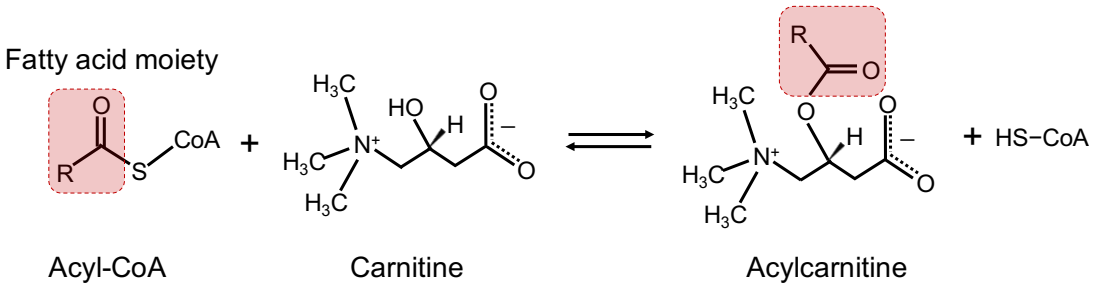

Figure 2.7. The reaction where acylcarnitine is formed from an acyl-CoA and a free carnitine molecule.

2.2 Lipid function in biological systems

All the different lipids described in detail in the previous section have important functions within biological systems and they are the most abundant lipids in the systems studies in the work in this thesis, neuron-like cells and heart tissue. Their structural variety provides them with different functions and in the this section their particular function within the systems cellular membranes and heart tissue, are described in more detail.

2.2.1 Lipids as cell membrane components

The cell membrane (or plasma membrane) is a membrane that surrounds the cytoplasm of a cell. It provides structural integrity and mainly consist of proteins and glycerophospholipids (Figure 2.8) [60]. The phospholipids are an important component of the cellular membrane. Due to their hydrophobic fatty acid tails that are repelled by water, and their polar headgroup they form bilayer structures within an aqueous environment. The bilayer protects the interior of the cell while keeping the cell structurally flexible. One of the main functions of proteins in the membrane is to assist in transferring molecules across the membrane. Hydrophobic proteins are inserted into the hydrophobic environment in the center of the bilayer. Some proteins consist of both hydrophobic and hydrophilic amino acids, creating transmembrane proteins where the hydrophobic amino acids associate with the fatty acids tails of the lipids and the hydrophilic amino acids prefer interaction with the polar headgroups. The lipids and proteins together form a highly dynamic structure [60].

Lipids and proteins can diffuse freely in the plane of the membrane. This provides flexibility and the ability to rapidly adapt to changes in the outer environment. The ability for lipids to diffuse is dependent on the fluidity of the membrane which in turn is controlled by the lipid composition [61]. A high amount of saturated fatty acid tails creates a structured bilayer with lower fluidity. When the membrane contains a higher amount of unsaturated fatty acids, with slightly bent tails due to the presence of double bonds, a more fluid membrane is formed. The fluidity of a membrane is important for its function and is therefore highly regulated by the cell. It has been shown that a change in membrane composition can occur in response to external stimuli that would cause a change in membrane fluidity, such as temperature, in a variety of cells and organisms [62–64]. Cholesterol also

plays a role in regulating the fluidity of membranes, by the close interaction of the hydrophobic part of the cholesterol molecule with the phospholipid fatty acid chains. This interaction stabilises the membrane making it less fluid, and also makes it more difficult for very small water soluble molecules to pass though the membrane [65]. Cholesterol is hypothesised to form hydrogen bonds with saturated fatty acids, creating structured domains within the membrane [66]. These highly structured domains, called lipid rafts, are high in cholesterol and sphingolipids as well as specific membrane proteins [67]. The fatty acid content in the lipid rafts is more saturated than the rest of the membrane allowing high packing density and structural organisation of the lipids. Lipid rafts are thought to be involved in regulating signal transduction, since they are rich in various membrane proteins involved in cell signalling. Changes in membrane composition can also play a role in cellular events where high curvature structures are needed, e.g. during fission and fusion events such as exocytosis. In these events high curvature domains need to form within the membrane. The different geometries of the phospholipids facilitate this formation by rearranging in such a way that conical shaped lipids, such as PE, PA and PI are enriched in the fusion pore site while the more cylindrically shaped lipids like PC are depleted. This has been shown in other high curvature events as well, such as the mating of the organism *Tetrahymena thermophilia* [68, 69].

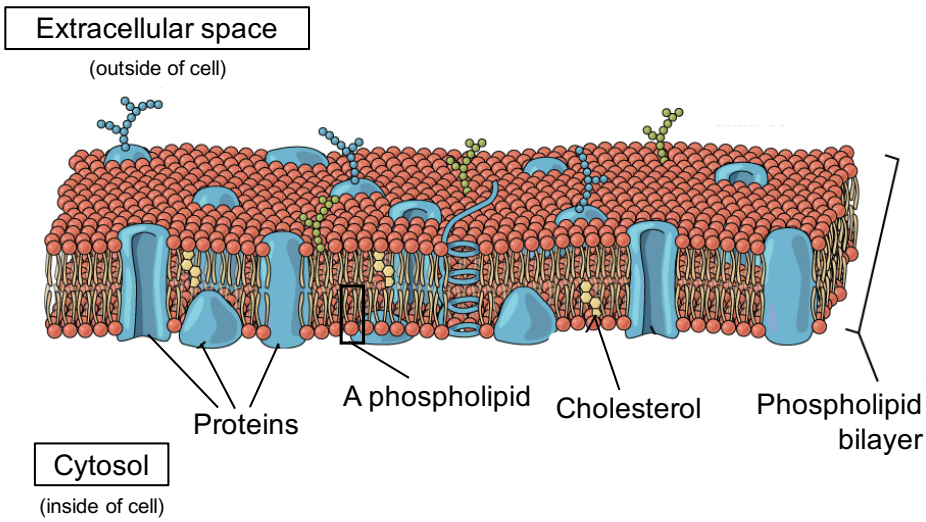

Figure 2.8. The composition of a cell membrane. Image credit: modified from OpenStax Biology [70].

Membrane lipids play an important role in many signalling pathways. Either by forming lipid rafts where accumulation of specific proteins can turn on and off sig-

nalling processes or by being important precursors of secondary messengers in many signalling pathways within the cell. Phosphoinositides are particularly important lipids [37]. Stimulation with a wide variety of signals (hormones, growth factors, etc.) causes activation of phospholipase C, an enzyme that hydrolyses phosphoinositide PIPs (phosphorylated PI species) to inositol triphosphate (IP_3) and diacylglyceride. IP_3 induces intracellular calcium release and can be further activated to other signalling molecules. Diacylglyceride is an activator of protein kinase C (PKC), which is an enzyme that takes part in signalling transduction cascades by phosphorylation of proteins. DAGs created from phospholipase C hydrolysis, are rapidly phosphorylated to form phosphatidic acid (PA). PA can bind to several signalling proteins, transducing the signal in the cascade [19]. DAGs and PA can also be generated by hydrolysis of PC lipids by phospholipase D, which generates species with a slightly different fatty acid content than when generated from phospholipase C hydrolysis of PIPs. Other active lipid species can be generated by the activation of phospholipase A, that creates lysolipids and fatty acids. Lysolipids is glycerophospholipids with one fatty acid tail making them conical in shape. When there is a high concentration of lysolipids they can perturb the membrane by creating small pore like features. Lysolipids more easily detach from the membrane and can therefore function as signalling molecules in the circulation system.

Other organelles within the cell are also surrounded by a lipid membrane. This includes the nucleus, endoplasmic reticulum, Golgi apparatus and the mitochondria. The lipid and protein composition of the various membranes vary with the function of the organelle [71]. For instance, the mitochondria has a double membrane structure with an outer and an inner membrane [72]. The outer layer resembles the plasma membrane in its phospholipid and protein content. It also contains porins, which are channel proteins, that allow diffusion of smaller molecules (less than 5000 Da) across the outer mitochondrial membrane. The function of this outer membrane is mainly to keep structural integrity [73]. Disruption of the outer membrane causes molecules from the inter-membrane space to leak into the cytoplasm initiating an apoptotic process. The inner membrane, however, resembles more a bacterial membrane with a high protein to lipid content. It also has a high concentration of cardiolipins [72], which is an important component for energy metabolism and also for forming a tight packing of the membrane to prevent diffusion of small molecules across the inner membrane. This creates a chemical barrier which is important for the energy metabolism process to function.

2.2.2 Lipids in heart tissue

The heart is one of the most energy requiring organs in the body. It utilises fatty acids as an energy source in order to create ATP. In a healthy human heart about 60-90% of the energy comes from β-oxidation of fatty acids, the rest of the energy comes from other substrates such as glucose, lactate and ketones [74]. β-oxidation is the catabolic process in which fatty acids are broken down to provide energy by forming products which can enter the citric acid cycle and the electron transport chain to create adenosin triphosphate (ATP), the cell's energy currency. This process requires oxygen. β-oxidation of fatty acids occurs on the inner membrane of mitochondria, so in order for ATP to be created the fatty acids need to be transported to and into the mitochondria in a series of steps (Figure 2.9). Studies have shown that the heart utilises both circulating free fatty acids and esterified fatty acids bound to lipoproteins [75]. Lipoproteins are an assembly of lipids and proteins designed for transporting hydrophobic lipids in the blood. They consist of an outer shell consisting of a single layer of phospholipids and cholesterol, specific proteins are embedded into the membrane to provide stability and guidance. The inside of the lipoprotein is packed with esterified fatty acids in the form of triacylglycerides, and these supply fatty acids to the heart *via* lipolysis. Very low density lipoprotein (VLDL) is the principal transporter of endogenous triglycerides. VLDL is secreted by the liver and has a high proportion of triglycerides but also contains cholesterol esters. Esterified FAs have been shown to be the major source of lipids for the human heart [76]. To first enter the cell, the fatty acids have to pass through specific membrane proteins. Once in the cytosol, they can be transported to the mitochondria by being transformed to a fatty acyl-CoA *via* the enzymatic reaction with a free Coenzyme A. When the fatty acyl-CoA reaches the outer membrane of the mitochondria, it cannot cross the hydrophobic membrane. For this to occur, the fatty acyl-CoA needs to react with a carnitine with the help of carnitine palmitoyltransferase I (CPT1) to form acylcarnitine. The acylcarnitine can be translocated into the inner membrane of the mitochondria at the same time as a carnitine is transfered to the outside by the action of carnitine-acylcarnitine translocase (CAT). Once inside the mitochondrial matrix, the acylcarnitine is converted back to fatty acyl-CoA witht the help of carnitine palmitoyltransferase II (CPT2) where it can take part in the β-oxidation process. During the β-oxidation, the fatty acid-CoA undergoes oxidative removal of two carbons in each step, creating acetyl-CoA. When the acetyl-CoA enters the citric acid cycle, there is a generation of $FADH_2$ and NADH, which are two coenzymes used in the electron transport chain to create ATP in a process that requires oxygen.

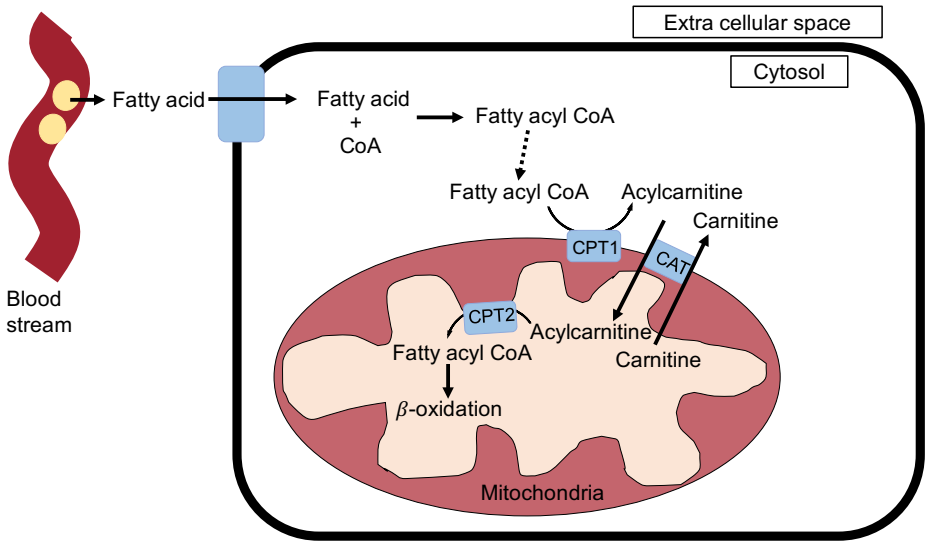

Figure 2.9. Schematic of the transportation process of fatty acids from the blood stream to the inner membrane of the mitochondria, where they take part in the β-oxidation process. The fatty acids have to go through a series of steps in order to reach the inner membrane of the mitochondria.

In most tissues, excess lipids are stored in lipid droplets. In healthy heart, not much lipid droplet accumulation can be detected indicating that the lipid uptake and β-oxidation process is highly regulated. In some circumstances, such as myocardial ischemia where oxygen supply is limited or when there is an increased workload in the heart, a rapid switch to glucose as a substrate for energy production occurs [77]. This leads to a reduced rate of β-oxidation of fatty acids. The highly regulated process between oxidation and lipid uptake is disrupted leading to an accumulation of lipids within the heart. Lipid accumulation has been detected in the ischemic heart, but can mainly be found in the border region between the ischemic and normal cardiac tissue, where a maximum amount of lipid droplets could be observed 6 hours after the infarction [78]. The lipid accumulation has been connected to the reduced rate of β-oxidation but it has also been shown that an increase in fatty acid uptake can be a contributing factor for accumulation [79]. Lipid accumulation following ischemia could also be due in part to increased lipid uptake via the VLDL receptor which is a membrane protein involved in the metabolism of TAG rich lipoproteins. Ischemia upregulates cardiac expression of the VLDL-receptor (Vldlr) that mediates uptake of triglyceride-rich lipoproteins. Vldlr deficient (-/-) mice showed improved survival and decreased infarct area following an induced myocardial infarction [80]. Accumulation of lipids in non-adipose tissue, that only has limited capacity for lipid storage, results in a cellular dysfunction called lipotoxicity. Lipotoxicity is

believed to be a contributing cause for impairment of heart function by instigating cardiac cell death among other things, although the exact mechanism of toxicity is not known since it has not been determined which lipid species accumulate [81]. Although, the accumulation has been associated with TAG species [82], as these are the cells natural form of storing excess lipids. However, TAGs are neutral lipids and are not thought to be responsible for the lipotoxicity, although some toxic effects of neutral droplets on myofibril function have been shown [83]. The toxic effects are more likely to arise from more reactive intermediates, such as fatty acids, DAGs and lysolipids. It is also believed that apoptosis can be initiated from saturated long-chain fatty acids [84], since they act as a substrate for the formation of ceramides, which are an apoptotic lipid signal for cells. Saturated fatty acids are also poor substrates for cardiolipin biosynthesis, leading to a decrease in the amount of mitochondrial cardiolipin content, causing cytochrome c, a vital enzyme in the electron transport chain, to release from the mithochondria which leads to initiation of apoptosis. DAGs and ceramides are both signalling lipids that are thought to be toxic when there is an increase in their intracellular concentrations. The toxic effect of ceramides has been observed by using a mouse model for cardiomyocyte death, where a reduction of ceramide levels, by inducing ceramidase, was shown do have beneficial effects [85]. Another possible toxin might be medium-chain acylcarnitines [86] or long-chain acylcarnitines [87], molecules that have shown to accumulate due to disruption of the carnitine fatty acid pathway in the mitochondria during ischemia.

2.3 Methods for studying lipids in biological systems

Lipids were for a long time considered to only be structural components in biological systems. In recent years, however, the diverse function of lipids has become clearer. Since lipids possess many important functions, as described in precious sections, they are essential targets for studies to better understand many biological processes. Their diverse structure and function, however, have made lipid analysis difficult and there is a lack of suitable techniques for lipid analysis compared to the amount of techniques existing for protein analysis.

For quantitative lipid analysis, methods such as thin-layer chromatography [88] and

high-performance liquid chromatography [89] have been employed where the lipids are seperated based on polarity. Also, enzyme-based fluorometric methods are being developed [24] in order to measure the amount of specific lipid species in different cells. For elucidating lipid structures, nuclear magnetic resonance spectroscopy can be used [90] where the spectra obtained are unique for each lipid species. The most common method for structure analysis however, is mass spectrometry (MS) . MS allows detection of small amounts of lipids in complex mixtures. This is usually done by extraction of lipids from cells or tissue by various extraction methods, and analysing the extracts with the help of MS. Lipid profiles can be gathered from various tissues or cells, and by comparing different extracts, identification of enhanced or depleted lipid species can done following different treatments or at different time-points [91]. Although analysing extracts from cells and tissues can be informative, this does not provide any spatial information since lipids from the entire cell/tissue are extracted. For studies where spatial information is collected using this type of analysis, isolation methods need to be improved.

Imaging methods provide another way to study the lipid composition of components in specific regions of cells/tissues. Fluorescent imaging has been used to study localisation and trafficking of lipids within living cells [92, 93]. Fluorescence experiments, however, require labelling with fluorescent tags that are usually very large compared to the lipid molecule. This could alter the structure and native behaviour of the lipid. Also, not enough fluorescent labels are commercially available for all lipid species and there is a limit to how many labels that can be used simultaneously. The drawback with using labels is also that prior knowledge of the analyte is needed.

Combining the mass spectrometry method to acquire chemical and structural information of the lipids, with imaging that provides spatial information, offers great potential for lipid studies. Time-of-flight secondary ion mass spectrometry (ToF-SIMS) imaging is a technique that has the capability to image lipids which allows for *in situ* lipidomics. Moreover, lipids provides an excellent analyte target for ToF-SIMS imaging due to the ionisation and sputtering properties of lipid species. Lipids are desorbed from the sample surface using a primary ion beam and also fall into the right mass-to-charge ratio to be analysed with ToF-SIMS, making lipids an optimal target. The next chapter discusses the mass spectrometry technique in general and describes the ToF-SIMS methodology in detail.

CHAPTER 3

Mass Spectrometry

3.1 General

Mass spectrometry has become one of the most widely used techniques among analytical methods. The characteristics of mass spectrometry, such as speed, sensitivity, detection limit and diverse use have given it an advantage over other techniques. The ability to use mass spectrometry for imaging has opened up exciting application areas for this technique, especially developments for imaging of biological samples have given new importance for this analytical technique.

Mass spectrometry can be described as an analytical technique that separates chemical compounds based on their mass-to-charge (m/z) ratio. It has a wide range of application areas as it can be used for identification of unknown compounds in a sample [94], relative quantification of a specific compound [95] or to elucidate the structure and chemical properties of different molecules [96]. There are a number of different mass spectrometers that are used today world wide in various applications areas, hence many different instrument configuration exist. However, three components are shared among most of the instruments; an ion source, a mass analyser and a detector in the configuration shown in Figure 3.1. The ion source converts part of the sample into gaseous ions. In the analyser, the ions are separated according to their mass-to-charge ratio and in the detector system the relative abundance of each ion is recorded. The signal from the detector is transmitted to a computer and the results are presented in a mass spectrum, usually with the mass-to-charge ratio on the x-axis and ion intensity or ion count on the y-axis. Most mass spectrometers function under high vacuum conditions to increase the mean free paths for the ions, which means that the they are able to travel long distances without colliding with another gas ion/molecule which would prevent them from reaching the detector, hence, reducing transmission. Mass spectrometry is usually a label free technique, which allows it to be applied as a so-called discovery technique as no prior knowledge of the target analyte is required.

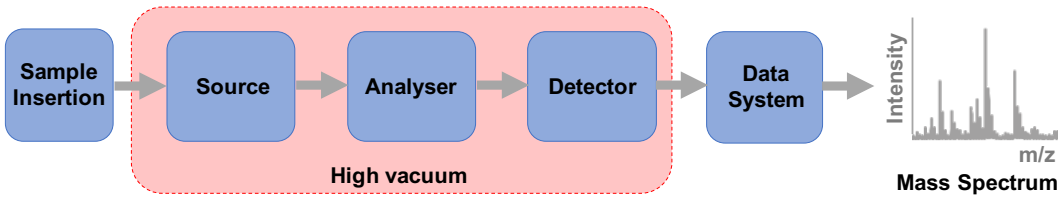

Figure 3.1. Basic components of a mass spectrometer.

As mentioned, there is a wide variety of different mass spectrometry instruments available on the market. Some combine the inlet and the ionisation source, some combine the mass separation with the detection system and there are others that can work at ambient pressures [97, 98]. The different instruments can apply either hard or soft ionisation techniques, where hard ionisation causes extensive fragmentation of molecules compared to soft ionisation where less fragmentation is observed. Soft ionisation techniques, such as matrix assisted laser desorption/ionisation (MALDI) [99, 100] and electrospray ionisation (ESI) [101], have greatly improved the ability for protein analysis in biological samples since higher mass species can be desorbed from the surface without fragmenting. The drawback with MALDI is that a matrix needs to be applied to the sample prior to analysis in order to desorb and ionise the analyte molecules, and the application of a matrix could lead to changes in the native sample surface. Also, lasers that are used for desorption of molecules during MALDI analysis, can be difficult to focus to small spot sizes which reduces the ability for chemical imaging at high spatial resolution. The work in thesis uses the ToF-SIMS technique, which falls into the hard ionisation category, where a focused ion beam is used for ionising and sputtering the analyte molecules off the surface of samples and the ions are then separated in a time-of-flight tube (ToF).

This chapter starts with a brief description of the history of the mass spectrometry technique, and later goes through the fundamentals of the ToF-SIMS technique in detail.

3.2 A brief history of mass spectrometry

The origin of mass spectrometry dates back to the end of the 19^{th} century. In 1897, JJ. Thompson developed an instrument, together with his lab assistant E. Everett,

that could measure the mass of fundamental particles, later named electrons, for which he was awarded the Nobel Prize in Physics in 1906 [102]. By using a cathode ray tube, which can produce a stream of electrons (also called cathode rays), he could determine the charge over mass ratio and the charge by studying how much the particles were bent when passed through an electrical field of varied strength. This provided an indirect measurement of the mass of the electron. Later, he also used the same instrument to study the mass of positively charged particles, cations [103].

FW. Aston, who was one of Thomson students, realised that a great deal of development could be done to the mass spectrometer with respect to the resolving power and mass range. He therefore developed a new mass analyser which he used to study the elements and managed to prove the existence of elemental isotopes [104, 105]. For this he was awarded the Nobel Prize in Chemistry in 1922.

To this point in history, the mass spectrometry technique was mainly used for fundamental research of atoms and particles. Hence, it was primarily a technique used by the physics community. It was A. Nier that helped "commercialise" the instrument and spread it to many different scientific fields. He designed and developed several new mass spectrometers which he used in a variety of different studies [106–108]. His work lead to many important publications, such as the measurement of the relative abundance of lead isotopes in the earth's crust which could later be used for estimating the age of the earth [109, 110]. He was also involved in finding the isotope of uranium responsible for nuclear fission [111] which was a critical step in the development of the first atomic bomb.

In the early 1950s, new types of instruments began to emerge, with different kinds of mass analysers that no longer used magnetic fields to separate the masses from each other. The quadrupole and ion trap mass analysers were developed and quickly became the most used types of analysers. The quadrupole was developed by W. Paul for which he recieved the Nobel Prize in Physics in 1989 [112, 113]. The concept of time-of-flight was introduced in 1946 by W.E. Stephens [114] and in 1948 the first time-of-flight (ToF) instrument was reported by Cameron and Eggers [115]. The time-of-flight analyser offered faster analysis time than the existing scanning instruments. Around this time mass spectrometers were also starting to be used in combination with other instrumentation creating gas chromatography mass spectrometry (GC-MS) [116, 117].

Secondary ion mass spectrometry (SIMS) was developed by R. Herzog and F. Viehböck [118] in the 1940s by creating a source that could provide separate accelerating fields for the primary and secondary ions. Static SIMS, where the density of the primary ion current is small enough to not damage the underlying layers, was introduced by A. Benninghoven in 1969 while looking at surfaces in ultra-high vacuum [119]. Initially, most of the static SIMS experiments were performed using Quadrupole mass analysers. However, in the mid-1980s it was realized that time-of-flight spectrometers are more efficient for this mode of SIMS, creating ToF-SIMS [120].

Up to this point, mass spectrometry was only able to study smaller molecules, and mainly used in the physics and chemistry fields. In the 1980s, two new ionisation sources were invented that revolutionised the mass spectrometry field, opening up possibilities for new applications; electrospray ionisation (ESI) [101] and matrix assisted laser desorption/ionisation (MALDI) [99]. These two techniques allowed for analysis of larger molecules making mass spectrometry very useful in the field of biology for analysis of proteins. The inventors of ESI and MALDI were awarded a part of the Nobel Prize in Chemistry in 2002 for their development of techniques that allowed the study of biological macromolecules.

In parallel, the SIMS imaging technique was developing. It started in the 60s with the invention of the "ion microscope" by R. Castaing and G. Slodzian [121]. Also, another way to image the sample by scanning the primary ion beam over the sample surface was developed around the same time. This was called an "ion microprobe". At the end of the 1960s, two instruments, one using the microscope technique and the other using the microprobe technique were commercialised. The microprobe instrument could reach 1 μm spatial resolution by focusing of the primary ion beam. In the 70s, the development of the liquid metal ion source made even smaller spot size possible, thus providing sub-micron spatial resolution.

In recent years, a lot of focus has been on development of new primary ion sources for improved spatial resolution or to generate higher secondary ion yields from molecular species. This has led to a variety of different sources used for imaging, such as Au_n^+, Bi_n^+, SF_5^+ and C_{60}^+. By optimizing the geometry of the instrument and using extensive apertures, a spot size of 50 nm was obtained in the CAMECA nanoSIMS instrument [122]. However, due to high fragmentation of the molecules during analysis only low mass ions are detected, which means isotope labelling is necessary for analysis of

molecular species. This is due to the fact that the smaller the spot size of the primary ion beam is, the higher is the amount of energy that is needed in order to desorb molecules from the sample. Higher energy causes higher fragmentation, which means that only low m/z are detected. In recent years, an interest has been to develop primary ion beams that allow analysis of higher molecular weight species with ToF-SIMS by using gas clusters as primary ions. The gas cluster ion beams (GCIBs) were first investigated as a method for modifying material surfaces [123] but were modified by J. Matsuo and coworkers for applications in SIMS [124]. The introduction of the GCIBs as a primary ion source have improved signals for higher mass species, but is still mainly used for etching of samples.

3.3 ToF-SIMS basics

ToF-SIMS is a mass spectrometry technique that combines a time-of-flight analyser with the secondary ion mass spectrometry ionisation method. It is a very surface sensitive technique that analyses the outermost layer of a sample. The ToF-SIMS technique combines the chemical specificity of mass spectrometry with the ability to image at high spatial resolution using a micro-focused energetic ion beam to ablate and ionise molecules from the sample surface.

3.3.1 Time-of-flight analyser

Time-of-flight (ToF) is an analyser used for separation of ions by utilising the fact that ions with the same kinetic energy but different mass-to-charge ratios have different flight times in a tube of known length. The ions created during the ionisation process get accelerated into the time-of-flight tube where they are separated as lighter ions travel faster than heavier ones. The relationship between the time it takes for an ion to travel through the tube and its mass-to-charge ratio can be derived from equations describing the potential and kinetic energy of the charged particles [115].

The potential energy of a charged particle in an electrical field can be described with the following equation,

$$E_p = qU \tag{3.1}$$

where E_p is potential energy for the particle, q is the charge of the particle and U is the strength of the electric field.

When the ions are accelerated into the time-of-flight tube the potential energy is converted to kinetic energy. The kinetic energy (E_k) of a particle of a certain mass is given by the equation,

$$E_k = \frac{1}{2}mv^2 \tag{3.2}$$

where m is the mass and v is the velocity of the particle.

Since all the potential energy gets converted into kinetic energy, Equation 3.1 and Equation 3.2 can be combined. By rearrangement and expressing velocity as distance divided by time,the following equation is produced,

$$t = \frac{d}{\sqrt{2U}}\sqrt{\frac{m}{q}} \tag{3.3}$$

where t is the time it takes for the ion (of mass m and charge q) to travel a specific distance d in an electric field with the strength U.

The values of d and U are instrument dependent and can in principle be set to a constant value k. Thus, equation 3.3 reduces to,

$$t = k\sqrt{\frac{m}{q}} \tag{3.4}$$

Equation 3.4 shows that the time it takes for an ion to travel trough a time-of-flight tubes depends on the square root of the mass-to-charge ratio.

In this derivation it is assumed that all the ions start out with the same kinetic energy. Because of the nature of the ablation process, there will be a range of different kinetic energies of the ions ablated from the sample and due to sample topography not all ions will start at exactly the same position. To improve the effects caused by the initial energy spread of the ions that leads to a decrease in mass resolution, many ToFs are equipped with a reflectron, also know as an ”ion mirror” [125]. The most common reflectron consists of a series of evenly spaced electrode plates, usually located at the end of the time-of-flight tube [126]. The ion mirror reverses the travel direction of ions by applying an electric field which decelerates the ions to zero velocity and re-accelerates them in the opposite direction. This causes the travel path of each ion to increase, which allows for more time for ions of different m/z

to spread out. The reflectron also corrects for the spread in kinetic energies of the ions as the ions with higher kinetic energy will penetrate deeper into the reflectron than the ions with lower energy, increasing their path length. This causes the ions with the same m/z but different kinetic energies and therefore velocities to reach the detector at the same time. The most common reflectrons use a linear electric field but other configurations exist where a non-linear field is used [127, 128]. On the J105 instrument (described in detail in Chapter 4.3), for example, a non-linear field reflectron is used which allows ions to be separated due to their mass-to-charge ratios independent of their kinetic energies.

The major advantage of a ToF analyser is that parallel ion detection is possible. Since the ions arrive at the detector sequentially, detection of all ions that were present in the source can be accomplished. Other analysers that use scanning techniques allow only one or a few species to be analysed at the same time and a mass spectrum is created by scanning over a mass range [113]. This is why ToF instruments have high sensitivity and higher throughput compared to other systems where scanning is needed. Also, analysis is rapid and allows for detection of a wide mass range. The mass accuracy can be better than 5 ppm and mass resolution ($m/\Delta m$) around 10,000 or even as high as 80,000 can be acheived [129]. However, with conventional ToF-SIMS instruments, an interlaboratory study has shown that the mass accuracy readily obtained is around 150 ppm [130].

3.3.2 Fundamentals of secondary ion mass spectrometry

In SIMS, a surface is bombarded with a focused beam of energetic primary particles, so called primary ions. Generally when the primary ions hit the sample surface, their energy is transferred to atoms in the sample *via* atomic collisions and a so-called collision cascade is generated, where atoms in the sample transfer the collision energy to other atoms [131]. Part of the energy is transported back to the surface allowing surface atoms and molecules to overcome the surface binding energy, thus, get released (sputtered) from the surface (Figure 3.2). Most of the emitted particles are neutral in charge (around 99%), but a small proportion are positively or negatively charged and it is these charged "secondary" ions that are collected and analysed.

SIMS is a very surface sensitive technique because generally the emitted particles

originate from the uppermost one or two monolayers and the particles are emitted within an area of a few nm in diameter from the primary ion impact site. There are a wide variety of primary ions that can be used such as atomic ions (Ar^+, Ga^+, Cs^+), polyatomic ions (Au_n^+, Bi_n^+, SF_5^+, C_{60}^+, where n=1-5) and gas cluster ions (Ar_n^+ and $(CO_2)_n^+$, where n is several thousands).

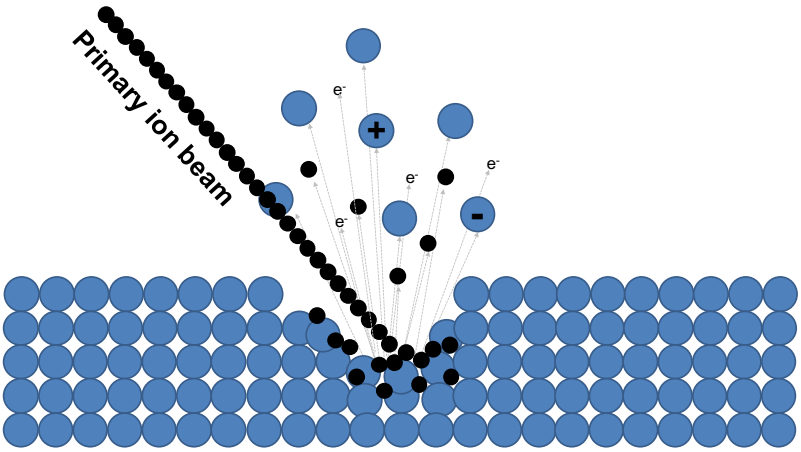

Figure 3.2. Schematic of the sputtering process in ToF-SIMS. Focused high energy primary ions bombard the sample causing particles and secondary ions to leave the sample surface.

3.4 Dynamic *versus* static SIMS

The use of high energy primary ion beams causes rapid removal of material from the surface. It also causes damage and modification to the underlying layers due to ion implantation, mixing of atoms and heavy fragmentation of molecules. This mode of SIMS, where a high primary ion dose is used, is called dynamic SIMS. It was the main mode of operation in the early days of SIMS until around 1980s. The dynamic SIMS method is useful for analysis of chemical composition of materials as a function of depth as it sputters away material during analysis providing information about not only the upper most surface but also the bulk material in the sample. In dynamic SIMS, the surface is eroded by sputtering with a continious primary ion beam with energies ranging from 0.25 keV to 50 keV. Due to heavy fragmentation it is primarily elemental information that can be obtained from the sample and not molecular information. The main application areas for dynamic SIMS have been in geological sciences [132, 133] and in microelectronics where semiconductor analysis

is performed in order to characterise elemental contamination [134]. In recent years, the use of the dynamic SIMS mode for 3D analysis of biological samples has been investigated and proven useful [135, 136].

At the end of the 1960s, a new mode of running SIMS analysis was introduced by A. Benninghoven [119]. Using lower primary ion doses for analysis resulted in fewer primary ions hitting the sample surface, thus causing less modification and less damage to the surface. This also led to less fragmentation which meant that molecular information could be obtained from the surface [137]. This mode of operation was named static SIMS. Static SIMS offers unique possibilities since monolayer sensitivity is combined with the capability to generate molecular information. It can be used for chemical composition analysis of native surfaces which is useful in many areas within material science.

Dynamic and static SIMS can be separated by the primary ion dose acceptable for analysis. For the static SIMS mode, no primary ion should hit an area that has already been damaged by another primary ion. When low primary ion doses are used the probability of primary ions striking the same area more than once is very low. During the time scale of the experiment only about 1% of the surface layer should be impacted by an ion to be defined as static mode. Taking into account that an area of about 10 nm^2 is influenced during impact of one ion, this means that the primary ion dose must be $\leq 10^{13}$ ions/cm^2 for static SIMS. This limit is called the static limit and varies depending on beam and sample type.

The primary ion dose can be calculated by using the following equation,

$$\text{Primary ion dose} = \frac{I_p t}{A} \tag{3.5}$$

where I_p is primary ion of flux (ions/s), t is the analysis time (s) and A is the surface area (commonly in cm^2) being analysed.

3.5 SIMS equation

The number of secondary ions available for detection during the analysis process depends on several parameters and the relationship between them is described in the following equation:

$$I_{m^{\pm}} = I_p Y_m \alpha_m^{\pm} \theta_m \eta \tag{3.6}$$

where $I_{m^{\pm}}$ is the secondary ion current of charged species m (in counts per second), I_p is the current of the primary ions (in ions/s), Y_m is the sputter yield of species m, $\alpha_m^{\pm}$ is the ionisation probability of species m, θ_m is the fractional concentration of species m in the surface layer, η is the transmission of the analyser system.

Equation 3.6 shows that the number of secondary ions of the charged species m (the analyte) that are available for analysis is linear depending on a number of factors. I_p is limited by the requirement of the primary ion dose for static SIMS to be below the static limit when maintaining of surface integrity is required, whereas the fractional surface concentration of species, m, is an intrinsic value of the sample, leaving the sputter yield, Y_m, and ionisation probability, $\alpha_m^{\pm}$, as the two significant parameters that determine how well a species can be analysed during SIMS. The transmission, η, is specific for each instrument design.

3.5.1 Sputter yield

During the SIMS process, primary ions hit the sample surface causing ejection of material from the outermost layer of the sample. The particles sputtered from the surface are neutral species, electrons, and positively and negatively charged ions (Figure 3.2). The sputter yield, Y_m, is defined as the number of secondary analyte particles (m), neutral and ionic, sputtered by one primary particle. The sputter yield increases with the mass and energy of the primary particle and it is also dependent on the incident angle of the primary ions. The sputter yield can also depend on the sample and will be effected by the crystallinity and topography of the sample.

For monatomic beams, the energy of the primary ions affects the sputter yield with higher energy leading to higher yield. The energy threshold of the primary particles for sputtering to occur is around 20-40 eV. Below this, there is not enough energy for the sputtering process to take place and no molecules will leave the surface. If the energy is too high, above 50 keV, the primary particle will penetrate so deep into the sample that no energy will return to the surface, hence, no sputtering will occur. The sputter yield is also effected by the mass of the primary ions. The larger the mass of the primary particle the closer to the surface the energy will be deposited. When the energy is deposited close to the surface, a higher sputter yield is obtained. The smaller the mass the primary ions have, the deeper they can penetrate which

will lead to lower sputter yield.

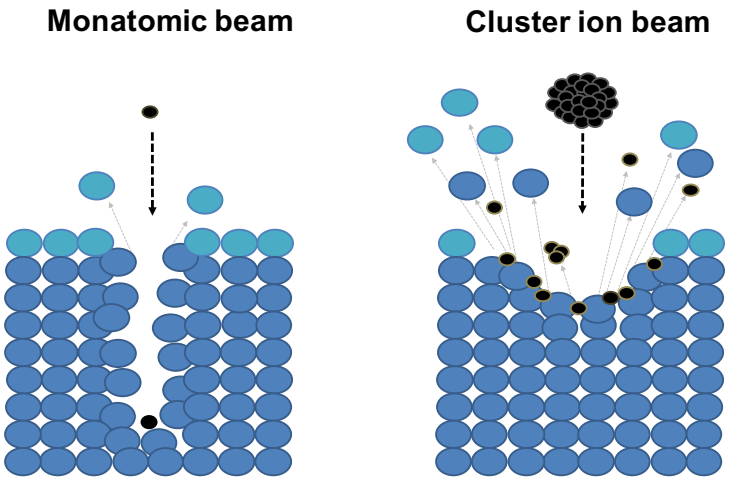

Figure 3.3. Comparison of a monatomic and a cluster ion beam, showing the difference in sputter yield observed when the number of atoms in the beam increases.

The development of polyatomic beams, such as SF_5^+ and C_{60}^+, and gas cluster ion beams (such as Ar_n, where n can be several thousands) have been shown to give an enhancement in the observed sputter yield. This is believed to be due to reduced depth of the energy deposited since the masses of the polyatoms and clusters are higher than for single atom beams. For polyatomic and cluster ion beams, the energy of the beam is spread over all the atoms in the cluster. This means that when the cluster breaks apart upon impact with the surface, each atom will have a fairly low amount of energy causing less penetration and damage to underlying layers but since many atoms will impact the surface, more material will be sputtered away (Figure 3.3). However, it has been shown that if the energy of the C_{60}^+ is below 10 keV, deposition of C_{60} can occur on the surface [138]. For argon cluster ion guns, no apparent inclusion of argon atoms can be seen meaning that there is less damage and no need for the argon beam to sputter its own deposit. For argon cluster ion guns, it was shown that the sputter yield increased by a factor of 10 for cluster ion beams at 20 keV, when compared to an argon monatomic beam at the same energy [139, 140]. Multiple practical and theoretical studies have been performed to investigate how the energy per nucleon (E/n) of the cluster affects the sputter yield and in some cases the ionisation of the analyte. A general observation is that for $E/n > 10$ eV a linear dependency of sputter yield with E is observed with only a weak influence of n. Below 10 eV/n, non-linearity is observed in secondary ion

yield when the ionisation efficiency is reduced as shown by Angerer *et al.* where on Irganox 1010 Ar^+_{4000} produced less than 50% secondary ion yield (ca. 20%) at 20 kV accelerating potential versus 40 kV despite a measured 50% reduction in sputter rate [141]. As *E/n* decreases a sputtering threshold is reached. This can manifest as either complete cessation of sputtering, or preferential sputtering as reported by Moritani *et al.*. During the analysis of polystyrene, main chain fragment signal decreased relative to side chain fragments when *E/n* decreased below 5 eV [142]. A similar effect was reported by Angerer *et al.* on cholesterol, where the $[M\text{-}H]^+$ decreases relative to the $[M+H\text{-}H2O]^+$ with decreasing *E/n*. Such observations suggest the possibility of using GCIBs to perform mass *spectroscopy*.

3.5.2 Ionisation probability

Only about 1% of the sputtered particles are ionised during the sputtering process. Whether a sputtered particle escapes from the surface as an ion depends on the ionisation probability, $\alpha^{\pm}$, of that specific species. It also depends on the electronic and chemical state of the surrounding material, the matrix. For analysis of organic molecules, the detection efficiency in SIMS is usually low due to low ionisation probability which sometimes is as low as 10^{-5}. The exact mechanism of how the ionisation occurs during the SIMS process is not known; however, models have been developed in order to describe what factors influence the ionisation process during SIMS, such as the charge transfer model [143].

Ionisation is believed to occur at, or close to, the surface during the desorption process. This means that not only the electronic state of the atom or the molecule to be ionised is important but also the electronic state of the matrix from which the ions are emitted. Some evidence suggests that the ions detected come from already pre-formed ions existing on the sample surface, together with a counter-ion. However, this does not explain the observation for all the omitted ions. One hypothesis is that any neutral molecule desorbed from the surface can react with an electron or a desorbed ion in the near surface area, to form ions. This also means that acid-base reactions could occur in the gas phase, making gas-phase basisity an important factor determining protonation/deprotonation events, hence, also effecting ionisation probability. For organic analysis in SIMS, molecular ions can be generated. Here, secondary ion formation can occur through a number of mechanisms for these molecules, where the most common are acid-base reactions (formation of $[M+H]^+$ and $[M\text{-}H]^-$ ions) or cat- or anionisation of neutral molecules, which will

form ions such as $[M+Na]^+$, $[M+K]^+$ and $[M+Cl]^-$.

As mentioned previously, the ionisation probability of a species can vary depending on the chemical environment in the sample. This phenomenon, coupled with local variation in sputter yield, is called the matrix effect. In SIMS, as with other desorption ionisation methods, this constitutes a major hurdle for quantitative analysis since the amount of ions detected for a specific species can either be enhanced or suppressed depending on the surrounding material. Hence, SIMS can only be considered a semi-quantitative technique.

As already stated, the detection efficiency for organic molecules is low owning to low ionisation probabilities, hence, there have been many attempts to increase the secondary ion yield by increasing the ionisation probability. Analysing samples in a frozen hydrated state has shown an increase in the formation of $[M+H]^+$ ions as water provides a proton source. The presence of electronegative species, such as oxygen, at at the surface could also greatly enhance ionisation potential. The ionisation efficiency can also depend on and be improved by the choice of primary ion beam. The use of dynamic reactive ionisation, by doping reactive molecules (such as HCl) into argon cluster ion beams, has been shown to increase protonation of neutral species [144]. It also has been shown to reduce matrix effects caused by salt. The use of water clusters as primary ions also resulted in increased secondary ion yields compared to argon clusters [145], believed to be due to higher ionisation probabilities. The use of cesium vapour also increases secondary ion yield in negative ion mode [146] however this might be caused by reduced fragmentation and charging effects not changes in ionisation efficiancy. Matrix enhanced SIMS, with the addition of a matrix on the sample, can also enhance molecular secondary ion yields [147] . Laser post ionisation (LPI), where the sputtered species are being hit with a laser to increase ionisation of species, has also been attempted and leads to an increase in secondary ion yields [148]. In paper III, included in this thesis, sodium chloride solution was applied on the sample, which provided a more even salt matrix across the sample, hence more $[M+Na]^+$ was identified.

3.6 ToF-SIMS imaging

ToF-SIMS is a well suited method for imaging since the primary ion beams can be focused to very small spot sizes, thus allowing imaging at high spatial resolution.

Primary ion beams have been focused down to 50 nm (nanoSIMS) but are normally used between 100 nm and 1 μm. An advantage that mass spectrometry imaging has over other imaging methods is that no prior knowledge of a sample is needed and in most cases no labelling of the wanted analyte is required. This means that it is suitable as a discovery technique for analysis of unknown samples. In fluorescent imaging, good spatial resolution can be achieved but there is a need for fluorescent labelling of the analyte and therefore prior information of the sample is needed. In imaging techniques like scanning electron microscopy (SEM), imaging at very high spatial resolutions can be achieved but chemical information provided is limited. This gives ToF-SIMS an unique place among imaging techniques.

Two different modes for ToF-SIMS imaging have been developed, the microprobe mode and the microscope mode. In the microprobe mode, the ion beam is rastered over the sample surface, collecting one mass spectrum at each pixel point. By plotting the intensity of a specific peak in the mass spectrum in every pixel, a chemical map of that compound can be generated (Figure 3.4). In this mode, the spatial resolution is dependent on how small the primary ion beam can be focused to. The microscope mode uses a defocused primary ion beam instead. The beam size used for adsorption of molecules/ions from the surface is usually around 200-300 μm. Secondary ions are generated over a large area, and are transported through the mass spectrometer with preserved spatial distribution. The secondary ions are detected using position-sensitive detectors [149]. In this mode, the analysis speed is greatly increased since no scanning of each pixel point is needed [150]. The spatial resolution is also decoupled from the ionisation sourse and instead dependent on the performance of the position-sensitive detectors. The latest advances in microscope mode mass spectrometry imaging use pixelated detectors, where every pixel act as an individual detector, making it possible to obtain spatial- and time resolved ion images simultaniously [151].

ToF-SIMS also provides the ability to carry out 3D imaging. The 3D images can be acquired using a few different approaches. The first is to image a series of consecutive slices of a sample in 2D. Fiducial markers are usually used to align the images together, and the 2D images can be fused together into a 3D image reconstruction of the sample [152]. Another approach is to use an ion beam to gradually erode the sample. This approach can provide depth resolutions in the order of several nm and is routinely employed in the semi-conductor industry. On ToF-SIMS instruments, 3D imaging normally employs alternating etching and analysis cycles,

where the ion beam is pulsed to generate mass resolved signal during analysis and fired continuously for etching the sample between analyses. Alternatively, a dual beam approach can be adopted where a different analysis beam compared to the etching beam is used. In dual beam mode, the analysis beam (usually a liquid metal ion gun which can be focused to small spot sizes) creates a 2D image of the surface. The sputter beam is then used for removal of a few layers of material from the surface, before the analysis beam is used again to acquire a new 2D image of the sample. The stack of 2D images can then be fused together, with the help of imaging software, to create a 3D image [135, 136, 153]. For organic/biological analysis, the etching beam is normally a polyatomic or gas cluster beam (e.g. C_{60}^{+} or Ar_{2000}^{+}, respectively) that can remove the sub-surface damage caused by the metal cluster (normally Bi_3^{+}/Au_3^{+}) analysis beam. A drawback of this approach is that the chemical information between the layers is lost. However, recent advances in instrumentation have allowed cluster ion beams to be used as analysis beams at the same time as material is being sputtered away due to an increase in sputter yield and reduced damage cross section [141] . In this approach, information is not lost since all the material is being analysed in the instrument and a nano-meter depth resolution can be achieved [154].

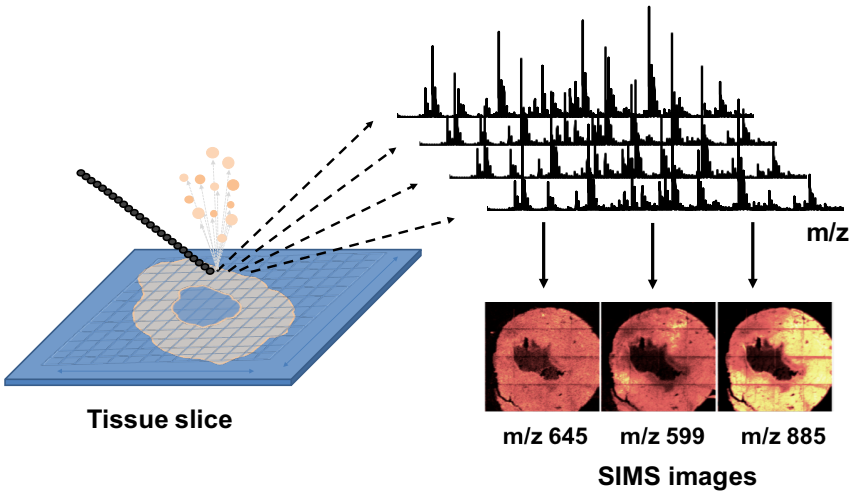

Figure 3.4. Schematic showing the microprobe imaging mode for ToF-SIMS imaging. A focused primary ion beam ablates material from a pixel point on the sample. By collecting one spectrum for each pixel point, the intensity for each ion can be plotted, creating chemical maps (SIMS images).

3.7 Biological applications for ToF-SIMS imaging

Biological material presents a great challenge for imaging experiments due the complex nature of the sample, where a mix of different types of molecules is present in the sample at the same time. They also contain a large portion of water which is usually not compatible with high vacuum techniques like ToF-SIMS. However, different sample preparation techniques have been developed for ToF-SIMS analysis that has allows for analysis of these types of samples (discussed in more detail in Chapter 4.2). Also, with the development of polyatomic and cluster ion beams such as C_{60}^{+} and gas cluster ion beams (GCIBs), it has become easier to detect higher mass species which has made ToF-SIMS imaging more useful for biological applications. In the recent decade, ToF-SIMS has been shown to be a useful technique for imaging of a variety of biological samples. As previously mentioned, lipids are an optimal target for ToF-SIMS imaging due to the ionisation and sputtering properties of lipid species and also their appropriate mass-to-charge ratio. Therefore, many studies of biological samples have focused on the lipid composition in various samples of tissues, cells, and bacteria. In this section, some ToF-SIMS studies for biological applications are presented to show the possibilities of the technique on various samples.

ToF-SIMS imaging has been used on a variety of different tissues in order to, for example, elucidate lipid changes during pathological processes or other types of tissue damage. ToF-SIMS imaging has been applied to Alzheimer's diseased brains since an increase in specific lipid species such as cholesterol in the brain has been correlated with this condition. Cholesterol is a good target for ToF-SIMS imaging making it a desirable method to use. In a study performed on human brains, the distribution of cholesterol in the cerebral cortex was mapped out and an increase of cholesterol in the grey matter was found compared to control brains [155]. Another study used ToF-SIMS imaging together with other imaging methods such as histology and fluorescence to image brain slices from an Alzheimer's diseased mouse model [156]. They found that cholesterol was located in close proximity to the alpha beta plaques that accumulate as a part of the pathology process in Alzheimer's. ToF-SIMS is especially useful when applied together with other methods to elucidate biological processes in tissues. MALDI-ToF and cluster-ToF-SIMS imaging have been applied together on skin and kidney tissue sections from patients suffering

from Fabry disease, a disease that causes accumulation of specific toxic lipids. Due to the ability to image the distribution of most lipids simultaneously in ToF-SIMS, the study provided a better understanding of the biological processes underlying Fabry disease by studying the distribution of not only the toxic lipids but other lipids as well [157]. In breast cancer tissue, the use of a novel high energy GCIB showed elevated levels of essential lipids related to inflammatory cells, whereas cancerous areas were higher in nonessental fatty acids, indicating that cancer cells have the ability for *de novo* biosynthesis of lipids [158]. ToF-SIMS imaging of lipid distribution in the brain of *Drosophila melanogaster* (fruit fly) after oral administration of methylphenidate, an effective treatment for children suffering from attention deficit/hyperactivity disorder, showed changes both in the amount and distribution of various lipid species that might be connected to damage of the nervous system [159].

Due to the high spatial resolution offered by the focused ion beams, imaging of smaller features such as cells, can be successfully performed. The first 3D biomolecular ToF-SIMS imaging was performed on *Xenopus laevis* oocyte, showing the distribution of various lipid species in three dimensions [135]. Time course sampling, revealed lipid remodelling during fertilization and early embryo development and the lipid distribution on the gamete fusion site was revealed [160]. Imaging of mating *Tetrahymena thermophila* with ToF-SIMS revealed that low curvature lipids were depleted in places where highly curved fusion pores exist, suggesting that heterogeneous redistribution of lipids could help in initiation of fusion events [68, 69]. The effect of silver nanoparticles on cell membrane composition of human macrophages has also been studied with ToF-SIMS. Characteristic changes in the lipid pattern of the outer leaflet of the cellular membrane were induced by the nanoparticles, but could be partially reversed trough treatment with *N*-acetyl cysteine, which is a molecule used as a diatery supplement [161].

ToF-SIMS imaging has also been applied to bacterial cells in different studies. Imaging of bacteria is a challenge due to their small size, usually around 1 μm. This challenge can be overcome by looking at clusters of bacteria, instead of single bacterial cells or by using depth profiling since the ToF-SIMS has nanometer depth resolution [154]. In a study by Winnograd *et al.*, images of bacteria were acquired that had been treated with two different kinds of antibiotics that had been shown to locate to different intracellular compartments [162]. In this study a C_{60}^+ ion beam with a 300 nm beam size was used for imaging. Depth profiling revealed that one

of the antibiotics was only located to a depth of 400 nm into the bacteria, whereas the other one was found in the cell interior. This shows that ToF-SIMS is useful for tracking the intracellular accumulation of exogenous compounds inside very small comparments such as bacteria. In another bacterial study, a 40 keV GCIB has been employed to investigate membrane lipid modifications as a result of starvation stress in the bacteria strain *E. coli* [163]. Here, a wild-type strain was compared to a strain that lackes stress response due to a specific mutation. It was found that the wild-type *E. coli* reacted upon carbon starvation by the onset of lipid modifications including elongation, cyclopropanation, and increased cardiolipin formation. In the mutant, the lipid modification such as elongation and desaturation of fatty acid chains was still found to occur, whereas cyclopropanation was not detected, indicating that the cycloproponation is a stress response that the bacterial cell keeps under stringent control. ToF-SIMS has also been applied together with other techniques in a high troughput microarray to determine the attachment of specific bacterial species to different polymeric materials in order to find materials that reduce bacterial attachment and biofilm formation [164].

In the work in this thesis, the ToF-SIMS imaging technique has been applied on both tissue and cell samples in order to elucidate lipid changes in both types of samples. Next chapter describes the specific methodologies used in this work in more detail as well as the biological samples used.

CHAPTER 4

Methodology

4.1 Model organisms

In this thesis, two different model organism have been used in order to study lipid composition related to different processes. For studying changes in lipid composition in heart tissue after a myocardial infarction, an induced myocardial infarction mouse model has been used (papers II, III and IV). For the cell studies, PC12 cells have been used to assess membrane lipid changes after incubation with fatty acids (paper V). In this chapter, the specific models are discussed as well as sample preparation, data analysis methods and the ToF-SIMS instrument used.

4.1.1 Surgically induced myocardial infarction

Cardiovascular disease is the leading cause of death in many developed countries and the most common among these is coronary heart disease. Coronary heart disease is a group of diseases, commonly characterised by build up of plaques on the inside of the coronary arteries, leading to limitations of blood flow to the heart. A myocardial infarction (MI), commonly referred to as a heart attack, is caused by a complete blockage of one of the coronary arteries supplying oxygen and nutrients to the heart. This causes ischemia in parts of the heart tissue which leads to necrosis. If the MI causes damage to a large part of the heart, it could ultimately lead to heart failure. Due to the severe implication of a MI and that it is so commonly occurring, it has been an important target of investigation in order to develop cardioprotective therapies. It is necessary to understand the pathophyshiological mechanism in the cardiac tissue following an infarction, therefore the development of animal models that mimic the pathology is essential. Various strategies and methods have been developed such as induction of hypercholesterolemia, which is a build up of plaques leading to narrowing or blockage of the arteries due to high fat diets [165, 166]. Although this approach mimicks the pathology, the time and site of the occlusion is random causing difficulty in producing reproducible experimental conditions. However, development of methods for surgically inducing a myocardial infarction

have led to the ability to precisely control the timing and location of the occlusion, leading to more reproducible results. This method has been applied to a number of different animals, like pigs [167], dogs [168] and rats [169]. The most common approach in recent years has been the use of mice as model organisms [170, 171]. They are easy to genetically modify and therefore a wide variety of mouse models for different diseases exist. The occlusion can be temporary or permanent, depending on the focus of the study. For examination of the short-term consequences of ischemic injury, temporary occlusions can be performed, whereas permanent occlusion is usually used for investigation of myocardial changes such as remodelling that occur over an extended period of time.

In papers II, III and IV, a surgically induced myocardial infarction mouse model using a permanent occlusion was used in order to study the lipid distribution within the heart following the infarction.

4.1.2 PC12 cells

PC12 cells are a cell line derived from a pheochromocytoma (a neuroendocrine tumor) of the rat adrenal gland [172]. They can be differentiated into neuron-like cells using nerve growth factor (NGF) or dexamethasone. They share properties similar to neurons by releasing neurotransmitters from vesicles. They are easy to maintain in culture and can be readily transfected and are therefore a common cell line to use to study the neurotransmitter release process and the neuronal differentiation process. This cell line is widely used as *in vitro* model of dopaminergic cells. PC12 cells have also been used in a variety of studies of changes in cell membrane lipid composition during different processes, for example, manganese treatment which was shown to induce apoptosis due to modifications of the lipid composition of the cell membrane [173]; changes in lipid composition which altered the susceptibility of PC12 cells to oxidative stress [174]; and fatty acid modification, which was shown to change the ability of PC12 neurite outgrowth formation [175].

In paper V, PC12 cells were used to investigate changes in membrane composition after incubation with the essential fatty acids, omega-3 and omega-6, by utilising isotopically labelled lipids.

4.2 Sample preparation for ToF-SIMS analysis

The ToF-SIMS technique is an ultra-high vacuum technique which requires samples to be vacuum compatible. This is a problem when analysing biological samples since they normally contain a large amount of water. A variety of preparation techniques have been developed in order to preserve the chemical and spatial integrity of the surface at the same time that the sample is made vacuum compatible [176]. A common method in other high vacuum imaging techniques, such as scanning electron microscopy, is chemical fixation where the sample is fixed with e.g. glutaraldehyde and then dried. This preserves the structural integrity of the sample; however, it might change its native chemical composition and water soluble species likely migrate during the procedure. This makes it a poor preparation method for SIMS analysis. Some groups have sucessfully used chemical fixation for 2D analysis of cells [177] but concluded that the method was not sufficient for cell membrane analysis.

A different fixation method, cryofixation, where samples are snap frozen and analysed either frozen or freeze-dried, is a more useful method for SIMS analysis [178]. Analysing the dry sample simplifies the handling of the sample; however, prior to drying, the removal of excess salts and media residues from cell cultures is needed to avoid accumulation of salt on the sample surface, which will interfere during analysis. Washing in volatile buffers, such as ammonium formate, has been used to maintain cell structure while removing salts [179]. Freeze-drying of samples can, however, also cause migration of species during the drying procedure. Changes in the distribution of ions attributed to DAG species have been reported in fly brain samples [180] and cholesterol migration have been observed on brain tissue slices [181, 182] and mouse heart tissue slices [183] during freeze-frying procedure. However, the effect of cholesterol migration can be overcome by sample exposure to trifluoroacetic acid (TFA) vapour [184].

Another aspect in cryofixation is that water changes to ice during freezing, which could alter the cell morphology by formation of ice crystals. Considerable effort has been put into developing rapid freezing methods (plunge freezing) or using high pressure (high pressure freezing) to avoid large crystal formation. During rapid freezing a sample is plunged into a cryogen cooled down by liquid nitrogen. The

cryogen should have a low boiling point and high thermal conductivity for rapid cooling to occur. Plunge freezing in liquid ethane has shown good preservation of cell structures and compatibility for lipid analysis [185].

Instrumental developments have led to analysis of frozen samples without the need for a freeze-drying step. Frozen hydrated analysis adds additional complexity to the sample preparation where it is important to minimise ice deposition on the surface of the sample that might mask biological signals due to the surface sensitivity of the ToF-SIMS technique. Instrumental design to insert samples without contact with air minimises surface ice formation. Other approaches have been the use freeze fracture devices, where cells are trapped between two slides and subsequently plunge frozen. Once inside the instrument the slides are forced apart by the fracturing device, exposing the cells. This approach minimises the ice interference, but the fracture planes produced are not always reproducible [186]. The ice layer formed can also be removed by using controlled heating of sample [187]. Frozen hydrated analysis have been shown to improve the signal for protonated ions since protons are readily provided from the water matrix [188].

In paper II, freeze-dried and frozen hydrated sample preparation protocols are compared for heart tissue slices and frozen hydrated sample analysis are shown to provide higher signal in both positive and negative ion mode. For cell analysis, in paper I and paper V, the cells were freeze-dried after being plunge frozen in isopentane cooled down by liquid nitrogen.

4.3 ToF-SIMS analysis with the J105

While the development of new ion beams have improved the ability to detect higher mass species, they were found to not be well suited for use together with standard time-of-flight analyser systems optimised for high sensitivity analysis in the static mode. This has lead to the development of new instrumental designs better optimised for these new ion beams. Various approaches have been used, including adaptation of a C_{60}^{+} ion gun to fit on a "Q-Star" MALDI mass spectrometer [189]. Also, instruments have been adapted or designed to provide higher mass resolution for accurate biochemical identification [190, 191]. All ToF-SIMS experiments in the papers included in this thesis were performed using a J105 - *3D Chemical Imager*, designed to be used with polyatomic or GCIBs. the instrument is descried in detail

in this section.

The J105 ToF-SIMS instrument was developed in collaboration between the University of Manchester (UK) and Ionoptika Ltd. (Southampton, UK) [192]. It was developed in order to decouple the mass resolution with the spatial resolution, as well as to optimise the instrumental set-up for organic/biological sample analysis [193]. In conventional ToF-SIMS instruments, the primary ion beam is pulsed in order to create tight packets of secondary ions that can be time resolved in the time-of-flight tube. Short pulses are necessary to achieve good mass resolution, but this also means that the signal needs to be collected over a larger area to get enough signal. When imaging at higher spatial resolution with low primary ion current, longer pulses are needed to collect enough signal in a practical time frame, thus compromising the mass resolution.

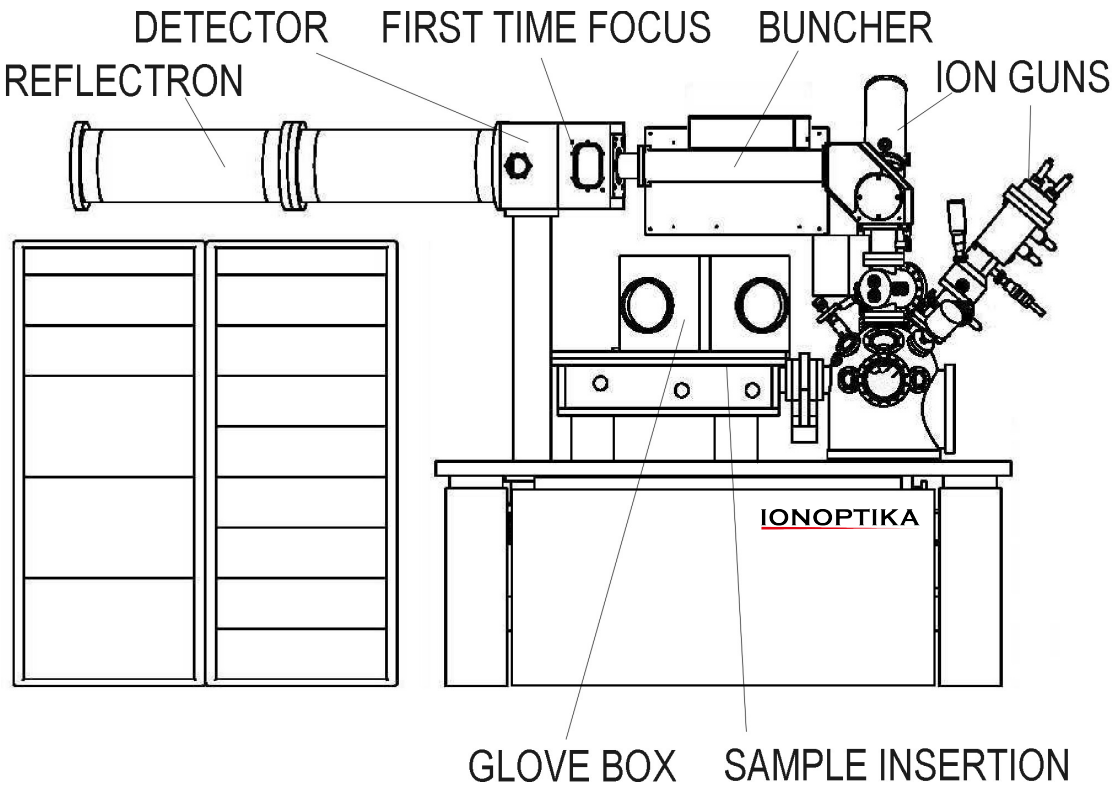

Figure 4.1. Schematic of the J105 - *3D Chemical Imager*. Image reproduced and adapted with permission from Fletcher *et al.* [193].

The J105, uses a continuous primary ion beam and it is instead the secondary ions that are bunched together in tight packets before entering the ToF tube, the schematic of the instrument can be seen in Figure 4.1. In more detail, the primary

ion beam hits the sample surface, producing a continuous stream of secondary ions. The secondary ions are extracted into a radio frequency-only quadrupole filled with a suitable gas (e.g. N_2) for collisional cooling and are then energy filtered by an electrostatic analyser. The resulting secondary ions now have an energy spread of about 1 eV before injection into a linear buncher (Figure 4.2). When the buncher fires, by applying an accelerating field on the buncher plates, the secondary ions are bunched together in a tight spot at a time focus at the entrance of the time-of-flight tube. The buncher plate field varies from 6 keV on the plates at the entrance of the buncher to 0.5 keV on the plates at the exit, allowing bunching of the ions. The acceleration in the buncher provides the ions with an energy spread of about 6 keV. Conventional ToF-SIMS instruments uses linear reflectrons, but they are not compatible with the large energy spread created by the buncher. The J105 utilises a non-linear field ToF reflectron, and the mass analyser of the J105 incorporates only a very short field free region between the buncher and the reflectron in order to perform ToF-ToF MSMS (Figure 4.2). The mass resolution is dependent on the performance of the buncher and is decoupled from the sputtering process. The current buncher setup can achieve a mass resolution of about 7000 at m/z 700-800 and a mass accuracy of 5 ppm. The instrument in our laboratory is equipped with a 40 keV C_{60}^+ ion gun and a 40 keV GCIB. The C_{60}^+ can be focused to under 1 μm and the GCIB can be focused down to about 3 μm for Ar_{4000}^+ [141].

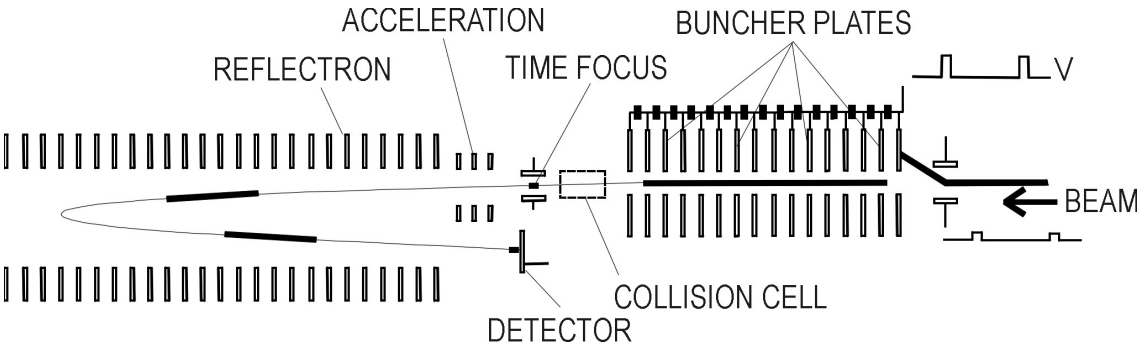

Figure 4.2. Schematic of the buncher and ToF configuration on the J105. Image reproduced and adapted with permission from Fletcher *et al.* [193].

The J105 is optimal for biological sample analysis since it is equipped with a glovebox mounted over the sample insertion port that can be filled with inert gas (e.g. argon), which allows for insertion of frozen samples without being in contact with air. The instrument sample stages can also be cooled down with liquid nitrogen, which permits frozen hydrated analysis to be performed.

Another feature is the MSMS capability. During MSMS analysis, ions exiting the buncher pass trough a collision cell filled with a suitable gas. The collisional energy, between the ions and the gas, is in the range of 1-7 keV since the collision cell is placed after the buncher. The species fragment, and since the collision takes place in a field free region, both the parent and daughter ions continue travelling with the same velocity. A timed ion gate is then used to select the ions of interest that then passes to the ToF analyser.

4.4 Multivariate analysis

During collection of ToF-SIMS images, a large amount of data is acquired. In ToF-SIMS imaging one mass spectrum is collected for every pixel point, and every mass spectrum consists of many mass channels corresponding to real peaks but also background peaks. With the large amount of data collected, it can be difficult to interpret, especially when analysing complex biological samples that contain a mixture of many different compounds. Multivariate analysis (MVA) of ToF-SIMS data has proven useful for reducing the amount of information collected to obtain relevant chemical information of the sample [194–196]. Two MVA methods that have been applied to ToF-SIMS images are principal components analysis (PCA) and maximum autocorrelation factor (MAF) analysis .

PCA is a technique that helps bring out strong patterns in the dataset by analysing the variance in the data. It reduces the dimensions of the data for easier interpretation, without losing a lot of information. In PCA, a n-dimensional ellipsoid is fitted to the data measured over n variables, where the axes of the ellipsoid represents the principal components (Figure 4.3a). The axis capturing the most variance is defined as principal component 1 (PC 1) and the succeeding components with decreasing variance are labelled PC 2, PC 3, etc. The result is usually presented in a 2- or 3D plot where the scores of the data points in each component are plotted. Data points clustering together in the score plot can be interpreted as sharing similar chemistry. In a loading plot, the mass peaks responsible for the similarities or differences in scores can be visualised. In PCA imaging, the pixels exhibiting similar chemistry according to the principal component scores will be given the same colour, revealing chemically similar areas in the image (Figure 4.3b). The loading plot will again show which peak contribute to that difference (Figure 4.3c). The PCA procedure

is sensitive to the scaling of the data, and a variety of different scaling can be used depending on the data set.

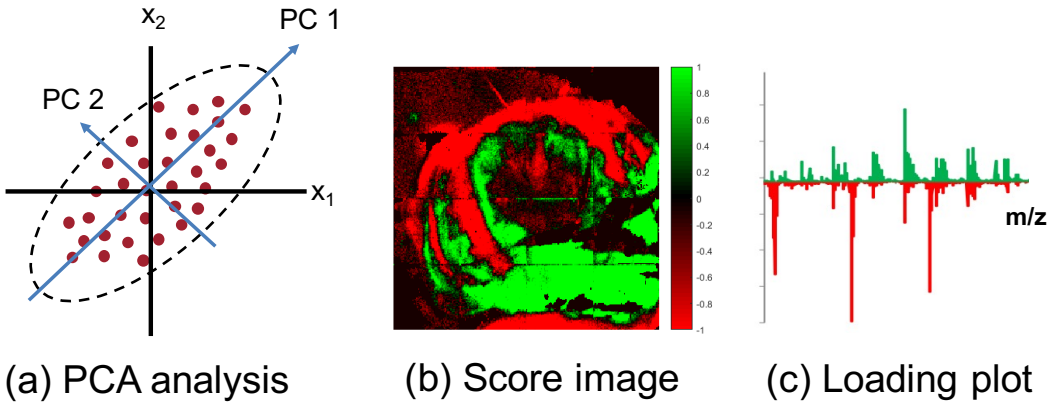

Figure 4.3. (a) Two dimensional representation of principal component analysis where an ellipsoid is fitted to the data measured over two variables, x_1 and x_2 and the axis capturing the most variance is labelled PC 1, (b) A score image showing pixels sharing similar chemistry in the same colour, (c) A loading plot showing which m/z contribute the scores in the score image.

MAF analysis is a multivariate analysis technique based on PCA; however, it correlates data in the space domain as well as mass domain which makes it suitable for analysing images. The analysis procedure maximises the autocorrelation between neighbouring pixels in an image, where interesting signals have high correlation and noise components have low correlation. As in PCA, the data is transformed into different components, called factors, and similar scoring pixels are plotted in the same colour. MAF analysis has been shown to be particularly useful for analysing image data as it is independent of scaling of the data, and so, no additional pre-processing steps are required [197–199].

In paper II, PCA and MAF analysis are compared on heart tissue slices and it was shown that for detection of small features in the image, MAF was the best choice. However, both PCA and MAF were found useful for identifying the lipid difference between the infarcted and the healthy region within the heart tissue.

CHAPTER 5

Summary of papers

The overall aim of this thesis has been to expand the application areas of the ToF-SIMS imaging technique for lipid analysis of biological samples, by either employing new instrument designs, development of new sample preparation methods, or by analysis of biological samples that previously have not been analysed using ToF-SIMS. In these investigations, both cells and tissue samples have been analysed by utilising a high energy gas cluster ion beam (40 keV GCIB) that has been shown to give enhanced signals for higher mass species such as intact lipids. The works has resulted in five papers that are summarised in this chapter.

In **paper I**, the possibility of using caesium flooding in combination with either a C_{60}^+ ion beam or a GCIB, to enhance the secondary ion yield, is investigated. It has previously been shown that caesium flooding can enhance secondary ion yield when using monatomic ion beams, but the application of caesium flooding together with cluster ion beams has not been assessed. A caesium flooding system, initially designed at the Luxembourg Institute of Science and Technology (LIST), was modified and mounted on a J105 instrument. The caesium vapour deposition was controlled by heating the caesium reservoir and the tube guiding the vapour. The enhancement of secondary ion yield was assessed on silicon, polycarbonate, and cells. Enhancement of the negative secondary ion yield is observed when caesium flooding is used with both C_{60}^+ and Ar_{4000}^+ ion beams for all analysed materials. Enhancement is observed for specific m/z during cell analysis, but higher deposition rates are needed for optimisation, something that was not possible to obtain with the current instrument design and could be a target for future work.

In **paper II**, a possible application area of a GCIB for ToF-SIMS imaging of tissue is evaluated. Cardiac tissue from the mouse is imaged following a myocardial infarction, also known as a heart attack. The infarction was surgically induced by ligation of the left anterior descending coronary artery. This procedure causes ischemia in parts of the heart muscle, mimicking the pathology of a heart attack. Previous histological studies have shown lipid accumulation in the border region between the infarcted and non-infarcted region of the heart following a myocardial infarc-

tion using Oil-red-O staining that stains for neutral lipids. This lipid accumulation can lead to decreased heart function and ultimately cause heart failure. Therefore, knowledge of what types of lipids accumulate could aid in finding better treatment methods. For the study in paper II, an argon cluster ion beam was employed for imaging of the lipids in the cardiac tissue following an infarction. Both freeze-dried and frozen hydrated tissue samples were analysed to determine the optimal sample preparation methods for these samples. Due to surface migration of certain species such as cholesterol during the freeze-drying process, the intensity for higher mass signals was decreased in the freeze-dried samples compared to frozen hydrated samples. Therefore, frozen hydrated sample analysis, where the samples are kept in a frozen state throughout the analysis, was found to be the optimal preparation method. For data analysis, two different multivariate analysis methods were employed, principal components analysis (PCA) and maximum autocorrelation factor (MAF) analysis. A comparison showed that both PCA and MAF can be used for differentiating between the infarcted and non-infarcted (healthy) regions; however, analysis with MAF also reveals minor features that appear in the border region, something that did not occur with PCA. MAF images together with loading plots were used for identifying important lipids species related to the infarcted and non-infarcted regions. Individual ion images were created from the highest peaks in the loading plot, and the distribution of the lipids was compared to control samples, where no infarction was induced. Comparison shows that the infarcted (ischemic) tissue region is higher in sodium, while the non-infarcted region is higher in potassium. Many phosphoinositol (PI) species are also found to be depleted in infarcted region. The border region, between the infarcted and non-infarcted regions, is found to contain several highly localised acylcarnitine species. It is hypothesised that the accumulation of acylcarnitines indicates a change in energy utilisation by the heart during ischemic conditions. The results from the ToF-SIMS imaging analysis showed a good correlation with liquid-chromatography mass spectrometry (LC-MS) analysis, which also shows differences between the infarcted and non-infarcted region. However, with LC-MS analysis it was not possible to detect the smaller differences found in the border region, such as accumulation of acylcarnitines and some specific PI species. This shows the importance of the imaging experiment, where spatial information is collected, to detect highly localised differences.

To elucidate more long-term biochemical responses of the heart following an infarction, a follow up study was performed using the same mouse model as in paper II, but where the tissue was collected at longer time points after the infarction and the

results are presented in **paper IV**. In this study, it was found that the size of the infarction increased with time. Similar lipid composition as found in the study in paper II, was found in the infarcted area with a high sodium content and depletion of specific phosphatidylinositol species. Also, imaging of heart tissue at high spatial resolution revealed localisation of species connected to apoptotic signalling, such as phosphatidylserine and phosphatidic acid, in the same region as the lipid accumulation is observed during histology analysis. Being able to follow the progression of the infarction chemically, by applying ToF-SIMS imaging at different time points following the infarction, offered insights in tissue response to an hypoxic environment. The border region is the tissue in the front-line of the progressing infarction, hence, the changes occurring there, such as accumulation of specific species, can reveal the responses in the acute phase of the infarction while the changes in the infarcted region shows more long-term responses, such as depletion of phosphatidylinositols. Hence, by applying ToF-SIMS imaging of tissue at different time points, spatio-temporal information could obtained which allowed for better understanding of the breakdown process of the tissue.

During the heart analysis, it was found that some parts of the mass spectrum were difficult to interpret due the formation of diacylglyceride (DAG) like ions from fragmentation of triacylglyceride (TAG) species. The fragmentation peaks of TAGs overlap with the DAG peaks, making it impossible to differentiate between these two species. DAG and TAG share similar chemical structure; however, they possess very different functions within a cell. For correct biological interpretation of mass spectra, it is therefore important to be able to distinguish between these two species. In **paper III**, a simple method of salt addition to the sample as a way of distinguishing between DAG and TAG species is presented. Lipid standards of a DAG and a TAG were analysed in order to determine fragmentation patterns, without and in the presence of NaCl. The formation of a $[M+Na]^+$ ion is found in the DAG spectra with salt addition, which does not overlap with any peak from the TAG fragmentation pattern, which meant that this peak could be used for differentiation between the two different species. The method was evaluated on two different tissue samples, rat brain and mouse heart. On both tissue samples, salt was successfully added without any major migration of species or disruption in sample morphology. After salt addition, the majority of the DAG like ions are found to be fragments of TAG species and do not originate from native DAG species. During analysis of the heart tissue, other benefits with salt addition were also found. As shown in paper II, large differences in sodium are found between the infarcted and non-infarcted regions of

the heart tissue. The large salt difference makes it difficult to identify small differences in lipid composition in positive ion mode, since large matrix effects caused by the salt mask these. When NaCl is applied in an even layer over the heart tissue, the matrix effects are decreased and smaller differences in lipid saturation between the two different regions in the heart can be detected. Hence, salt addition was found to be a simple method that simplified spectra interpretation of complex tissue samples.

In **paper V**, another possible application area for ToF-SIMS was investigated where a GCIB and a liquid metal ion gun (LMIG) were used to track the incorporation of specific fatty acids into the plasma membrane of cells. The essential fatty acids, α-linolenic acid (FA(18:3)) belonging to the omega-3 family, and linoleic acid (FA(18:2)) belonging to the omega-6 family cannot be synthesised in the body and therefore need to be provided in the diet. These fatty acids functions as precursors for a series of omega-3 and omega-6 long chain polyunsaturated fatty acids (PUFAs) *via* a fatty acid synthesis process of desaturation and elongation reactions. Both omega-3 and omega-6 PUFAs have been shown to exhibit health benefits and an increase in the ratio between these have been shown to have beneficial effects for neurodegenerative diseases [200]. Studying the incorporation of these essential fatty acids into the cell membrane of neuron-like cells could be an important step in understanding the biochemical mechanisms behind these beneficial effects. In this study, PC12 cells were incubated with omega-3 and omega-6 fatty acids. To be able to track the incorporation into longer chain fatty acids and phospholipids in the cell membrane, deuterium labelled fatty acids were used. Lipid imaging of single cells was possible using the LMIG and the incorporation of the two fatty acids into the cell membrane could be observed. While the LMIG provided information on fatty acid species, the GCIB was able to provide information of which phospholipid species the fatty acids incorporated into. Both omega-3 and omega-6 was found to mainly incorporate into phosphatidylcholine, phosphatidylethanolamine and phoshatidylinositol species. Also, relative quantification of the lipids species showed that the omega-3 fatty acids are incorporated in higher amount than omega-6 fatty acids. This study showed by applying ToF-SIMS imaging using a GCIB on cell samples it was possible to track the incorporation of fatty acids into the cell membrane.

CHAPTER 6

Concluding remarks and outlook

The ToF-SIMS imaging technique has, over the years, become a standard technique for analysis of inorganic samples (e.g. in the semi-conductor industry). In recent years, new instrumental designs together with the development of GCIBs as analysis beams have opened up new exciting application areas for the technique, however, there is still a need for further investigation of what types of sample could be used for analysis. The work in this thesis has aimed to investigate the use of ToF-SIMS imaging for lipid analysis of biological samples.

In this work, it was shown that using a caesium flooding system together with cluster ion beams enhances secondary ion signals when detecting negative ions and that there is potential for increased signal when using caesium flooding for analysis of cells. There is a need for further development of this approach but the results so far show that employing caesium flooding for biological imaging provides enhancement of secondary ion yields, which could be important during analysis of low abundance species. This could make it possible to analyse new types of samples previously not possible to analyse. It was also shown that using a simple experimental design where salt is applied on the sample prior to analysis can aid in interpretation of complex mass spectra from tissue samples. Differentiation between chemically similar species is accomplished with this simple sample preparation, and in the case of infarcted mouse heart tissue it also provides a more even matrix effect that reveals smaller differences in lipid distribution that can otherwise be masked by large differences in salt distribution across the sample. Development of techniques for better interpretation of complex mass spectra arising from analysis of biological samples makes it easier to use ToF-SIMS for biological applications.

As discussed in this thesis, an advantage of the ToF-SIMS technique is that the distribution of many lipids can be tracked at the same time without the need for labelling. Also, with new advances using the GCIB as an analysis beam, higher intensities for higher mass species can be detected making it possible to image intact lipid species. The ToF-SIMS technique is a surface sensitive technique that can be used to analyse the outer most layer of a sample. Thus, it can be employed

during analysis of the cell membrane. All of these advantages, provide a good basis for use of this technique for analysis of biological samples. The work in this thesis shows examples of two different biological systems that can be analysed using this technique where the analysis provides new important information of the two different systems. When applying ToF-SIMS imaging using a GCIB on heart tissue following a heart attack, spatial information of different lipid species within the infarcted heart can be collected. Specific lipids not detected in previously published conventional lipidomics studies are found with SIMS imaging to accumulate in the border region between healthy and infarcted heart tissue. The ability to collect spatial information of many lipids simultaneously during analysis is one of the main advantages of using the ToF-SIMS technique for these types of samples. The information gathered from these imaging studies provides more precise information of the biochemical changes occurring during breakdown and repair of heart tissue, which might aid in development of better treatment methods for patients suffering from a heart attack. Knowledge of which lipid species accumulate, and consequently causes impairment of heart function, provides new targets for development of drugs. These drugs could be designed to activate specific signalling pathways in the cells that removes or prevents the accumulation by break down or by incorporation of the toxic lipids into non-toxic species. Further, it was also shown that GCIB ToF-SIMS imaging is useful for tracking the incorporation of omega-3 and omega-6 fatty acids into the cell membrane. Employing this technique for cell membrane analysis can be useful for many different cell systems where information of the lipid changes occurring as a response to different stimuli or during disease pathologies might be useful for better understanding of various diseases and can also provide new insights in biochemical processes occurring within a single cell.

The work in this thesis shows the potential of ToF-SIMS imaging with GCIB to provide new information of various samples. In conclusion, this technique shows great promise for lipidomic analysis for biological applications and can be used as a complementary technique to other analysis methods routinely employed today.

CHAPTER 7

Acknowledgements

Doing a Ph.D. has been a great opportunity and also one of the greatest challenges of my life. It has been five difficult, exciting, frustrating, fun and educational years, and I have grown as a person both professionally and personally. This journey would not have been possible without all the people that have helped me throughout the years and I would like to take this opportunity to acknowledge some of them.

First of all, I would like to thank my supervisor **Andrew Ewing** for giving me the opportunity to do my Ph.D. in your research group. Thanks for believing in me and being so supportive through my studies. You have given me the freedom to pursue the research projects that I have found interesting, and your guidance have been of great help. The enthusiasm you show for science is inspirational.

I would also like to thank my co-supervisor **John Fletcher** for introducing me to the world of SIMS. You have taught me everything I know about the J105 and without your guidance a lot of the work in this thesis would not have been possible. I am very grateful for all the help you have provided through the years.

I would like to acknowledge all the co-authors of the papers included in this thesis. To the people at the Sahlgrenska University Hospital laboratory, who I have been collaborating with in the heart studies, **Jan Borén**, **Marcus Ståhlman**, **Martina Klevstig**, **Maria Heyden**. Thank you for an interesting collaboration and for providing great expertise when it comes to myocardial infarction. And a special thanks to **Mai Hoang Philipsen**, for a great collaboration on the fatty acid project, and for being so understanding in these stressful times.

Thanks to all the members (past and present) of the Ewing/Fletcher/Cans research groups for creating such a fun working environment. For all the interesting fika conversations, for the fun afterwork activities and for many fun conference trips. Working in such an international group have taught me new things about the world and about myself. I am happy to have met so many nice people during these past five years.

To my former office mate **Nhu Phan** for fun discussions and answering all my questions that I had in the beginning of my Ph.D, and to my current office mate **Mariia Pavlovksa**, for many interesting conversations, about nothing and everything and for all the great movie recommendation that have been greatly appreciated. I am happy that I got to share an office with you, it would have been very empty and boring without you!

Life is not only about work and I have had many people around me outside of work that have cheered me on in my pursuit of a Ph.D. degree. My friends and former classmates; **Niada**, **Emelie**, **Hanna** and **Linnea**. We have supported each other throughout our studies, but also through life's heartbreaks and happy times. Thanks for all the support, for always listening and understanding and for all the fun times we have shared. It is a privilege to have such amazing and smart women in my life! **Erika**, the first time i met you, you welcomed me into your home and from that moment on I have felt welcomed into your life. Thanks for listening to all my complaining without ever judging and for always understanding. Life can be tough sometimes, but I know we can handle whatever comes in our way. I am lucky to have found a friend like you. **Madde**, my oldest and closest friend who even though is far away, has always been there for me in so many ways. I know that wherever I am or whatever I do, you will be there routing for and supporting me no matter what. What would I do without you!

Henrik, you did not get to live your life very long but you are still with me everyday. You are my reminder that life is short, and there is no point on wasting it on things that does not make you happy.

My family, for always believing in me and supporting me in everything I do. This would not have been possible without you!

Dario, words can not describe how happy I am to have you in my life. This journey would not have been possible without your love and support. You are the wind blowing me in the right direction but you are also my rock, the steady place in my life that provides a soft place for me to fall. Also, seeing the hard work and dedication you put on trying to achieve your own goals is truly an inspiration for me. Thank you for being you, I love you! ♡

References

1. Passarelli, M. K. & Winograd, N. Lipid imaging with time-of-flight secondary ion mass spectrometry (ToF-SIMS). *Biochimica et Biophysica Acta (BBA)-Molecular and Cell Biology of Lipids* **1811,** 976–990 (2011).
2. Beloribi-Djefaflia, S., Vasseur, S. & Guillaumond, F. Lipid metabolic reprogramming in cancer cells. *Oncogenesis* **5,** e189–199 (2016).
3. Schulze, P. C. Myocardial lipid accumulation and lipotoxicity in heart failure. *Journal of Lipid Research* **50,** 2137–2138 (2009).
4. Lim, W. L. F., Martins, I. J. & Martins, R. N. The involvement of lipids in Alzheimer's disease. *Journal of Genetics and Genomics* **41,** 261–274 (2014).
5. Fahy, E., Cotter, D., Sud, M. & Subramaniam, S. Lipid classification, structures and tools. **1811,** 637–647 (2011).
6. Wakelam, M. J. Diacylglycerol–when is it an intracellular messenger? *Biochimica et Biophysica Acta (BBA)-Molecular and Cell Biology of Lipids* **1436,** 117–126 (1998).
7. Allen, W. Biochemical aspects of lipid storage and utilization in animals. *American Zoologist* **16,** 631–647 (1976).
8. Wolfman, A. & Macara, I. G. Elevated levels of diacylglycerol and decreased phorbol ester sensitivity in ras-transformed fibroblasts. *Nature* **325,** 359–361 (1987).
9. Shemesh, T., Luini, A., Malhotra, V., Burger, K. & Kozlov, M. Prefission Constriction of Golgi Tubular Carriers Driven by Local Lipid Metabolism: A Theoretical Model. *Biophysical Journal* **85,** 3813–3827 (2004).
10. Yang, C. & Kazanietz, M. G. Divergence and complexities in DAG signaling: looking beyond PKC. *Trends in Pharmacological Sciences* **24,** 602–608 (2003).
11. Brose, N., Betz, A. & Wegmeyer, H. Divergent and convergent signaling by the diacylglycerol second messenger pathway in mammals. *Current Opinion in Neurobiology* **14,** 328–340 (2004).

12. Ishizuka, T. *et al.* Glucose-induced synthesis of diacylglycerol de novo is associated with translocation (activation) of protein kinase C in rat adipocytes. *FEBS Letters* **249,** 234–238 (1989).

13. Zhang, L. *et al.* Cardiac diacylglycerol accumulation in high fat-fed mice is associated with impaired insulin-stimulated glucose oxidation. *Cardiovascular Research* **89,** 148–156 (2011).

14. Griner, E. M. & Kazanietz, M. G. Protein kinase C and other diacylglycerol effectors in cancer. *Nature Reviews Cancer* **7,** 281–294 (2007).

15. Meikle, P. J. *et al.* Plasma lipidomic analysis of stable and unstable coronary artery disease. *Arteriosclerosis, Thrombosis, and Vascular Biology* **31,** 2723–2732 (2011).

16. Miura, S. *et al.* Functional conservation for lipid storage droplet association among Perilipin, ADRP, and TIP47 (PAT)-related proteins in mammals, Drosophila, and Dictyostelium. *Journal of Biological Chemistry* **277,** 32253–32257 (2002).

17. Farese, R. & Walther, T. Lipid droplets finally get a little R-E-S-P-E-C-T. *Cell* **139,** 855–860 (2009).

18. Welti, R. *et al.* Profiling Membrane Lipids in Plant Stress Responses: Role of phospholipase Dα in freezing-induced lipid changes in Arabidopsis. *Journal of Biological Chemistry* **277,** 31994–32002 (2002).

19. Wang, X., Devaiah, S. P., Zhang, W. & Welti, R. Signaling functions of phosphatidic acid. *Progress in Lipid Research* **45,** 250–278 (2006).

20. Foster, D. A. & Xu, L. Phospholipase D in Cell Proliferation and Cancer. *Molecular Cancer Research* **1,** 789–800 (2003).

21. O'Luanaigh, N. *et al.* Continual production of phosphatidic acid by phospholipase D is essential for antigen-stimulated membrane ruffling in cultured mast cells. *Molecular Biology of the Cell* **13,** 3730–3746 (2002).

22. Huang, P., Altshuller, Y. M., Hou, J. C., Pessin, J. E. & Frohman, M. A. Insulin-stimulated plasma membrane fusion of Glut4 glucose transporter containing vesicles is regulated by phospholipase D1. *Molecular Biology of the Cell* **16,** 2614–2623 (2005).

23. Tan, B. K. *et al.* Discovery of a cardiolipin synthase utilizing phosphatidylethanolamine and phosphatidylglycerol as substrates. *Proceedings of the National Academy of Sciences* **109,** 16504–16509 (2012).

24. Morita, S. & Terada, T. Enzymatic measurement of phosphatidylglycerol and cardiolipin in cultured cells and mitochondria. *Scientific Reports* **5,** 11737–11752 (2015).

25. Eisenbrey, A. B. *et al.* Phosphatidylglycerol in amniotic fluid: comparison of an "ultrasensitive" immunologic assay with TLC and enzymatic assay. *American Journal of Clinical Pathology* **91,** 293–297 (1989).

26. Lombardi, F. J., Chen, S. L. & Fulco, A. J. A rapidly metabolizing pool of phosphatidylglycerol as a precursor of phosphatidylethanolamine and diglyceride in Bacillus megaterium. *Journal of Bacteriology* **141,** 626–634 (1980).

27. Jiang, F. *et al.* Absence of cardiolipin in the crd1 null mutant results in decreased mitochondrial membrane potential and reduced mitochondrial function. *Journal of Biological Chemistry* **275,** 22387–22394 (2000).

28. Thompson, T. & Tillack, T. W. Organization of glycosphingolipids in bilayers and plasma membranes of mammalian cells. *Annual Review of Biophysics and Biophysical Chemistry* **14,** 361–386 (1985).

29. Exton, J. Signaling through phosphatidylcholine breakdown. *Journal of Biological Chemistry* **265,** 1–4 (1990).

30. MacDonald, J. I. & Sprecher, H. Phospholipid fatty acid remodeling in mammalian cells. *Biochimica et Biophysica Acta (BBA)-Lipids and Lipid Metabolism* **1084,** 105–121 (1991).

31. Bance, J. Phosphatidylserine and Phosphatidylethanolamine in mammalian cells: two metabolically related aminophospholipids syndrome. *Journal of Lipid Research* **49,** 1377–1387 (2008).

32. Steenbergen, R. *et al.* Disruption of the phosphatidylserine decarboxylase gene in mice causes embryonic lethality and mitochondrial defects. *Journal of Biological Chemistry* **280,** 40032–40040 (2005).

33. Verkleij, A., Leunissen-Bijvelt, J., De Kruijff, B., Hope, M. t. & Cullis, P. *Non-Bilayer Structures in Membrane Fusion* in *Ciba Foundation Symposium 103-Cell Fusion* (2008).

34. Vance, J. E. & Tasseva, G. Formation and function of phosphatidylserine and phosphatidylethanolamine in mammalian cells. *Biochimica et Biophysica Acta (BBA)-Molecular and Cell Biology of Lipids* **1831,** 543–554 (2013).

35. Martin, S. *et al.* Early redistribution of plasma membrane phosphatidylserine is a general feature of apoptosis regardless of the initiating stimulus: inhibition by overexpression of Bcl-2 and Abl. *Journal of Experimental Medicine* **182,** 1545–1556 (1995).

36. Fadok, V. *et al.* Exposure of phosphatidylserine on the surface of apoptotic lymphocytes triggers specific recognition and removal by macrophages. *The Journal of Immunology* **148,** 2207–2216 (1992).

37. Di Paolo, G. & De Camilli, P. Phosphoinositides in cell regulation and membrane dynamics. *Nature* **443,** 651–657 (2006).

38. D'Souza, K. & Epand, R. M. Enrichment of phosphatidylinositols with specific acyl chains. *Biochimica et Biophysica Acta (BBA)-Biomembranes* **1838,** 1501–1508 (2014).

39. Imai, A. & Gershengorn, M. C. Independent phosphatidylinositol synthesis in pituitary plasma membrane and endoplasmic reticulum. *Nature* **325,** 726–728 (1987).

40. Chu, C. T. *et al.* Cardiolipin externalization to the outer mitochondrial membrane acts as an elimination signal for mitophagy in neuronal cells. *Nature Cell Biology* **15,** 1197–1205 (2013).

41. Hatch, G. M. Cardiolipin: biosynthesis, remodeling and trafficking in the heart and mammalian cells. *International Journal of Molecular Medicine* **1,** 33–74 (1998).

42. He, Q. & Han, X. Cardiolipin remodeling in diabetic heart. *Chemistry and Physics of Lipids* **179,** 75–81 (2014).

43. Sparagna, G. C. & Lesnefsky, E. J. Cardiolipin remodeling in the heart. *Journal of Cardiovascular Pharmacology* **53,** 290–301 (2009).

44. Schlame, M., Rua, D. & Greenberg, M. L. The biosynthesis and functional role of cardiolipin. *Progress in Lipid Research* **39,** 257–288 (2000).

45. Vandenheuvel, F. Study of biological structure at the molecular level with stereomodel projections I. The lipids in the myelin sheath of nerve. *Journal of the American Oil Chemists Society* **40,** 455–471 (1963).

46. Ruvolo, P. Ceramide regulates cellular homeostasis via diverse stress signaling pathways. *Leukemia* **15,** 1153–1160 (2001).

47. Coderch, L., López, O., de la Maza, A. & Parra, J. L. Ceramides and skin function. *American Journal of Clinical Dermatology* **4,** 107–129 (2003).

48. Fillet, M., Van Heugen, J.-C., Servais, A.-C., De Graeve, J. & Crommen, J. Separation, identification and quantitation of ceramides in human cancer cells by liquid chromatography–electrospray ionization tandem mass spectrometry. *Journal of Chromatography A* **949,** 225–233 (2002).

49. Haus, J. M. *et al.* Plasma ceramides are elevated in obese subjects with type 2 diabetes and correlate with the severity of insulin resistance. *Diabetes* **58,** 337–343 (2009).

50. De Mello, V. *et al.* Link between plasma ceramides, inflammation and insulin resistance: association with serum IL-6 concentration in patients with coronary heart disease. *Diabetologia* **52,** 2612–2615 (2009).

51. García-Ruiz, C., Colell, A., Marí, M., Morales, A. & Fernández-Checa, J. C. Direct effect of ceramide on the mitochondrial electron transport chain leads to generation of reactive oxygen species Role of mitochondrial glutathione. *Journal of Biological Chemistry* **272,** 11369–11377 (1997).

52. Ball, D., Hill, J. & Scott, R. *The Basics of General, Organic, and Biological Chemistry* (Saylor Academy, 2011).

53. Ohvo-Rekilä, H., Ramstedt, B., Leppimäki, P. & Slotte, J. P. Cholesterol interactions with phospholipids in membranes. *Progress in Lipid Research* **41,** 66–97 (2002).

54. Cooper, R. A. Influence of increased membrane cholesterol on membrane fluidity and cell function in human red blood cells. *Journal of Cellular Biochemistry* **8,** 413–430 (1978).

55. Schwartz, C. C. *et al.* Multicompartmental analysis of cholesterol metabolism in man: characterization of the hepatic bile acid and biliary cholesterol precursor sites. *The Journal of Clinical Investigation* **61,** 408–423 (1978).

56. Johnson, W. J., Mahlberg, F. H., Rothblat, G. H. & Phillips, M. C. Cholesterol transport between cells and high-density lipoproteins. *Biochimica et Biophysica Acta (BBA)-Lipids and Lipid Metabolism* **1085,** 273–298 (1991).

57. Pande, S. V. A mitochondrial carnitine acylcarnitine translocase system. *Proceedings of the National Academy of Sciences* **72,** 883–887 (1975).

58. Ramsay, R. R. & Tubbs, P. K. The mechanism of fatty acid uptake by heart mitochondria: An acylcarnitine-carnitine exchange. *FEBS letters* **54,** 21–25 (1975).

59. Rinaldo, P., Cowan, T. M. & Matern, D. Acylcarnitine profile analysis. *Genetics in Medicine* **10,** 151–156 (2008).

60. Singer, S. J. & Nicolson, G. L. The fluid mosaic model of the structure of cell membranes. *Science* **175,** 720–731 (1972).

61. Shinitzky, M. & Inbar, M. Microviscosity parameters and protein mobility in biological membranes. *Biochimica et Biophysica Acta (BBA)-Biomembranes* **433,** 133–149 (1976).

62. Murata, N. & Los, D. A. Membrane fluidity and temperature perception. *Plant Physiology* **115,** 875–879 (1997).

63. Cossins, A. & Prosser, C. Evolutionary adaptation of membranes to temperature. *Proceedings of the National Academy of Sciences* **75,** 2040–2043 (1978).

64. Martin, C. E. *et al.* Molecular control of membrane properties during temperature acclimation. Fatty acid desaturase regulation of membrane fluidity in acclimating Tetrahymena cells. *Biochemistry* **15,** 5218–5227 (1976).

65. Yeagle, P. L. Cholesterol and the cell membrane. *Biochimica et Biophysica Acta (BBA)-Reviews on Biomembranes* **822,** 267–287 (1985).

66. Edidin, M. Lipid microdomains in cell surface membranes. *Current Opinion in Structural Biology* **7,** 528–532 (1997).

67. Simons, K. & Ikonen, E. Functional rafts in cell membranes. *Nature* **387,** 569–572 (1997).

68. Ostrowski, S. G., Van Bell, C. T., Winograd, N. & Ewing, A. G. Mass spectrometric imaging of highly curved membranes during Tetrahymena mating. *Science* **305,** 71–73 (2004).

69. Kurczy, M. E. *et al.* Mass spectrometry imaging of mating Tetrahymena show that changes in cell morphology regulate lipid domain formation. *Proceedings of the National Academy of Sciences* **107,** 2751–2756 (2010).

70. Rye, C. *et al. Biology* (Openstax, 2016).

71. Van Meer, G., Voelker, D. R. & Feigenson, G. W. Membrane lipids: where they are and how they behave. *Nature Reviews Molecular Cell Biology* **9,** 112–124 (2008).

72. Hovius, R., Lambrechts, H., Nicolay, K. & de Kruijff, B. Improved methods to isolate and subfractionate rat liver mitochondria. Lipid composition of the inner and outer membrane. *Biochimica et Biophysica Acta (BBA)-Biomembranes* **1021,** 217–226 (1990).

73. Mannella, C. A. Structure of the outer mitochondrial membrane: ordered arrays of porelike subunits in outer-membrane fractions from Neurospora crassa mitochondria. *The Journal of Cell Biology* **94,** 680–687 (1982).

74. Taegtmeyer, H. Energy metabolism of the heart: from basic concepts to clinical applications applications. *Current Problems in Cardiology* **19,** 87–113 (1994).

75. Lopaschuk, G. D., Ussher, J. R., Folmes, C. D., Jaswal, J. S. & Stanley, W. C. Myocardial fatty acid metabolism in health and disease. *Physiological Reviews* **90,** 207–258 (2010).

76. Ballard, F. B., Danforth, W. H., Naegle, S. & Bing, R. J. Myocardial metabolism of fatty acids. *The Journal of Clinical Investigation* **39,** 717–723 (1960).

77. Ventura-Clapier, R., Garnier, A. & Veksler, V. Energy metabolism in heart failure. *The Journal of Physiology* **555,** 1–13 (2004).

78. Jodalen, H., Stangeland, L., Grong, K., Vik-Mo, H. & Lekven, J. Lipid accumulation in the myocardium during acute regional ischaemia in cats. *Journal of Molecular and Cellular Cardiology* **17,** 973–980 (1985).

79. Chabowski, A., Gorski, J., Calles-Escandon, J., Tandon, N. N. & Bonen, A. Hypoxia induced fatty acid transporter translocation increases fatty acid transport and contributes to lipid accumulation in the heart. *FEBS Letters* **580,** 3617–3623 (2006).

80. Perman, J. C. *et al.* The VLDL receptor promotes lipotoxicity and increases mortality in mice following an acute myocardial infarction. *The Journal of Clinical Investigation* **121,** 2625–2640 (2011).

81. Park, T.-S., Yamashita, H., Blaner, W. S. & Goldberg, I. J. Lipids in the heart: a source of fuel and a source of toxins. *Current Opinion in Lipidology* **18,** 277–282 (2007).

82. Bilheimer, D. W., Buja, L. M., Parkey, R. W., Bonte, F. J. & Willerson, J. T. Fatty Acid Accumulation and Abnormal Lipid Deposition in Peripheral and Border Zones of Experimental Myocardial Infarcts. *Journal of Nuclear Medicine* **19,** 276–283 (1978).

83. Finck, B. N. *et al.* A critical role for PPARα-mediated lipotoxicity in the pathogenesis of diabetic cardiomyopathy: modulation by dietary fat content. *Proceedings of the National Academy of Sciences* **100,** 1226–1231 (2003).

84. Borradaile, N. M. *et al.* A critical role for eukaryotic elongation factor 1A-1 in lipotoxic cell death. *Molecular Biology of the Cell* **17,** 770–778 (2006).

85. Holland, W. L. *et al.* Receptor-mediated activation of ceramidase activity initiates the pleiotropic actions of adiponectin. *Nature Medicine* **17,** 55–63 (2011).

86. Koves, T. R. *et al.* Mitochondrial overload and incomplete fatty acid oxidation contribute to skeletal muscle insulin resistance. *Cell Metabolism* **7,** 45–56 (2008).

87. Liepinsh, E. *et al.* Long-chain acylcarnitines determine ischaemia/reperfusion-induced damage in heart mitochondria. *Biochemical Journal* **473,** 1191–1202 (2016).

88. Rouser, G., Fleischer, S. & Yamamoto, A. Two dimensional thin layer chromatographic separation of polar lipids and determination of phospholipids by phosphorus analysis of spots. *Lipids* **5,** 494–496 (1970).

89. Christie, W. W. Rapid separation and quantification of lipid classes by high performance liquid chromatography and mass (light-scattering) detection. *Journal of Lipid Research* **26,** 507–512 (1985).

90. Gunstone, F. D. High resolution 13C NMR. A technique for the study of lipid structure and composition. *Progress in Lipid Research* **33,** 19–28 (1994).

91. Atilla-Gokcumen, G. E. *et al.* Dividing cells regulate their lipid composition and localization. *Cell* **156,** 428–439 (2014).

92. Kuerschner, L., Moessinger, C. & Thiele, C. Imaging of lipid biosynthesis: how a neutral lipid enters lipid droplets. *Traffic* **9,** 338–352 (2008).

93. Schütz, G. J., Kada, G., Pastushenko, V. P. & Schindler, H. Properties of lipid microdomains in a muscle cell membrane visualized by single molecule microscopy. *The EMBO Journal* **19,** 892–901 (2000).

94. Silverstein, R. M. & Bassler, G. C. Spectrometric identification of organic compounds. *Journal of Chemical Education* **39,** 546–553 (1962).

95. Ong, S.-E. & Mann, M. Mass spectrometry-based proteomics turns quantitative. *Nature Chemical Biology* **1,** 252–262 (2005).

96. Kind, T. & Fiehn, O. Advances in structure elucidation of small molecules using mass spectrometry. *Bioanalytical Reviews* **2,** 23–60 (2010).

97. Cooks, R. G., Ouyang, Z., Takats, Z. & Wiseman, J. M. Ambient mass spectrometry. *Science* **311,** 1566–1570 (2006).

98. Bruins, A. Mass spectrometry with ion sources operating at atmospheric pressure. *Mass Spectrometry Reviews* **10,** 53–77 (1991).

99. Tanaka, K. *et al.* Protein and polymer analyses up to m/z 100 000 by laser ionization time-of-flight mass spectrometry. *Rapid Communications in Mass Spectrometry* **2,** 151–153 (1988).

100. Karas, M., Bachmann, D., Bahr, U. & Hillenkamp, F. Matrix-assisted ultraviolet laser desorption of non-volatile compounds. *International Journal of Mass Spectrometry and Ion Processes* **78,** 53–68 (1987).

101. Whitehouse, C. M., Dreyer, R., Yamashita, M. & Fenn, J. Electrospray ionization for mass-spectrometry of large biomolecules. *Science* **246,** 64–71 (1989).

102. Thomson, J. J. XL. Cathode Rays. *The London, Edinburgh, and Dublin Philosophical Magazine and Journal of Science* **44,** 293–316 (1897).

103. Thomson., J. J. Rays of positive electricity and their application to chemical analyses. *Longmans, Green and Company* **1** (1921).

104. Aston, F. LXXIV. A positive ray spectrograph. *Philosophical Magazine* **38,** 707–714 (1919).

105. Aston, F. *Mass spectra and isotopes* (Esward Arnold, 1942).

106. Nier, A. O. A Mass-Spectrographic Study of the Isotopes of Hg, Xe, Kr, Be, I, As, and Cs. *Physical Review* **52,** 933–937 (1937).

107. Nier, A. O. A Mass Spectrometer for Routine Isotope Abundance Measurements. *Review of Scientific Instruments* **11,** 212–216 (1940).

108. Nier, A. O. & Gulbransen, E. A. Variations in the Relative Abundance of the Carbon Isotopes. *Journal of the American Chemical Society* **61,** 697–698 (1939).

109. Nier, A. O. Variations in the Relative Abundances of the Isotopes of Common Lead from Various Sources. *Journal of the American Chemical Society* **60,** 1571–1576 (1938).

110. Nier, A. O., Thompson, R. W. & Murphey, B. F. The Isotopic Constitution of Lead and the Measurement of Geological Time. III. *Physical Review* **60,** 112–116 (1941).

111. Nier, A. O., Booth, E. T., Dunning, J. R. & Grosse, A. V. Nuclear Fission of Separated Uranium Isotopes. *Physical Review* **57,** 546–546 (1940).

112. Paul, W. & Steinwedel, H. Ein neues massenspektrometer ohne magnetfeld. *Zeitschrift f r Naturforschung-A Journal of Physical Science* **8,** 448–450 (1953).

113. Hans-Peter, R., Heinz, F. & Wolfgang, P. *Method of separating ions of different specific charges* U.S. Patent 2,950,389. (1960).

114. Stephen, W. E. Proceedings of the American Physical Society. *Physical Review* **69,** 674–674 (1946).

115. Cameron, A. E. & Jr., D. F. E. An Ion "Velocitron". *Review of Scientific Instruments* **19,** 605–607 (1948).

116. McLafferty, F. W. Mass Spectrometry in Chemical Research and Production. *Applied Spectroscopy.* **11,** 148–156 (1957).

117. Gohlke, R. S. Time-of-flight mass spectrometry and gas-liquid partition chromatography. *Analytical Chemistry* **31,** 535–541 (1959).

118. Herzog, R. & Viehböck, F. Ion source for mass spectrography. *Physical Review* **76,** 855–856 (1949).

119. Benninghoven, A. Analysis of Submonolayers on Silver by Negative Secondary Ion Emission. *Physica Status Solidi (b)* **34,** K169–K171 (1969).

120. Chait, B. & Standing, K. A time-of-flight mass spectrometer for measurement of secondary ion mass spectra. *International Journal of Mass Spectrometry and Ion Physics* **40,** 185–193 (1981).

121. Castaing, R. & Slodzian, G. Optique corpusculaire-premiers essais de microanalyse par emission ionique secondaire. *Comptes Rendus Hebdomadaires Des Seances De L Academie Des Sciences* **255,** 1893 (1962).

122. Slodzian, G., Daigne, B., Girard, F., Boust, F. & Hillion, F. Scanning secondary ion analytical microscopy with parallel detection. *Biology of the Cell* **74,** 43–50 (1992).

123. Yamada, I. Investigation of ionized cluster beam bombardment and its applications for materials modification. *Radiation Effects and Defects in Solids* **124,** 69–80 (1992).

124. Yamada, I., Matsuo, J., Toyoda, N. & Kirkpatrick, A. Materials processing by gas cluster ion beams. *Materials Science and Engineering: R: Reports* **34,** 231–295 (2001).

125. Mamyrin, B., Karataev, V., Shmikk, D. & Zagulin, V. The mass-reflectron, a new non-magnetic time-of-flight mass spectrometer with high resolution. *Journal of Experimental and Theoretical Physics* **64,** 82–89 (1973).

126. Alikhanov, S. A new impulse technique for ion mass measurements. *Soviet Physics JETP* **4** (1957).

127. Cornish, T. J. & Cotter, R. J. *Non-linear field reflectron* U.S. Patent 5,464,985. (1995).

128. Cornish, T. J. & Cotter, R. J. A curved-field reflectron for improved energy focusing of product ions in time-of-flight mass spectrometry. *Rapid Communications in Mass Spectrometry* **7,** 1037–1040 (1993).

129. Satoh, T., Sato, T. & Tamura, J. Development of a high-performance MALDI-TOF mass spectrometer utilizing a spiral ion trajectory. *Journal of the American Society for Mass Spectrometry* **18,** 1318–1323 (2007).

130. Gilmore, I., Green, F. & Seah, M. Static TOF-SIMS. A VAMAS interlaboratory study. Part II–accuracy of the mass scale and G-SIMS compatibility. *Surface and Interface Analysis* **39,** 817–825 (2007).

131. Sigmund, P. *Sputtering by ion bombardment theoretical concepts* in *Topics in Applied Physics: Sputtering by particle bombardment I* (1981).

132. Dickinson, M. *et al.* Dynamic SIMS analysis of cryo-prepared biological and geological specimens. *Applied Surface Science* **252,** 6793–6796 (2006).

133. MacRae, N. D. Secondary-ion mass spectrometry and geology. *The Canadian Mineralogist* **33,** 219–236 (1995).

134. Chu, P. K. SIMS and microelectronics. *Materials Chemistry and Physics* **38,** 203–223 (1994).

135. Fletcher, J. S., Lockyer, N. P., Vaidyanathan, S. & Vickerman, J. C. ToF-SIMS 3D biomolecular imaging of Xenopus laevis oocytes using buckminsterfullerene (C60) primary ions. *Analytical Chemistry* **79,** 2199–2206 (2007).

136. Nygren, H., Hagenhoff, B., Malmberg, P., Nilsson, M. & Richter, K. Bioimaging ToF-SIMS: High resolution 3D imaging of single cells. *Microscopy Research and Technique* **70,** 969–974 (2007).

137. Steffens, P., Niehuis, E., Friese, T., Greifendorf, D. & Benninghoven, A. A time-of-flight mass spectrometer for static SIMS applications. *Journal of Vacuum Science & Technology A: Vacuum, Surfaces, and Films* **3,** 1322–1325 (1985).

138. Kozole, J. & Winograd, N. Controlling energy deposition during the C60+ bombardment of silicon: The effect of incident angle geometry. *Applied Surface Science* **255,** 886–889 (2008).

139. Matsuo, J., Toyoda, N., Akizuki, M. & Yamada, I. Sputtering of elemental metals by Ar cluster ions. *Nuclear Instruments and Methods in Physics Research Section B: Beam Interactions with Materials and Atoms* **121,** 459–463 (1997).

140. Seah, M. Universal equation for argon gas cluster sputtering yields. *The Journal of Physical Chemistry C* **117,** 12622–12632 (2013).

141. Angerer, T. B., Blenkinsopp, P. & Fletcher, J. S. High energy gas cluster ions for organic and biological analysis by time-of-flight secondary ion mass spectrometry. *International Journal of Mass Spectrometry* **377,** 591–598 (2015).

142. Moritani, K., Mukai, G., Hashinokuchi, M. & Mochiji, K. Site-Specific Fragmentation of Polystyrene Molecule Using Size-Selected Ar Gas Cluster Ion Beam. *Applied Physics Express* **2,** 0460011–0460013 (2009).

143. Lin, J. & Garrison, B. J. Charge transfer at surfaces: A model for ionization in SIMS. *Journal of Vacuum Science & Technology A: Vacuum, Surfaces, and Films* **1,** 1205–1208 (1983).

144. Tian, H., Wucher, A. & Winograd, N. Dynamic reactive ionization with cluster secondary ion mass spectrometry. *Journal of The American Society for Mass Spectrometry* **27,** 285–292 (2016).

145. Sheraz née Rabbani, S., Barber, A., Fletcher, J. S., Lockyer, N. P. & Vickerman, J. C. Enhancing secondary ion yields in time of flight-secondary ion mass spectrometry using water cluster primary beams. *Analytical Chemistry* **85,** 5654–5658 (2013).

146. Philipp, P. *et al.* Significant Enhancement of Negative Secondary Ion Yields by Cluster Ion Bombardment Combined with Cesium Flooding. *Analytical Chemistry* **87,** 10025–10032 (2015).

147. Wu, K. J. & Odom, R. W. Matrix-enhanced secondary ion mass spectrometry: a method for molecular analysis of solid surfaces. *Analytical Chemistry* **68,** 873–882 (1996).

148. Popczun, N. J., Breuer, L., Wucher, A. & Winograd, N. On the SIMS ionization probability of organic molecules. *Journal of The American Society for Mass Spectrometry* **28,** 1182–1191 (2017).

149. Luxembourg, S. L., Mize, T. H., McDonnell, L. A. & Heeren, R. M. High-spatial resolution mass spectrometric imaging of peptide and protein distributions on a surface. *Analytical Chemistry* **76,** 5339–5344 (2004).

150. Jungmann, J. H. *et al.* Fast, high resolution mass spectrometry imaging using a medipix pixelated detector. *Journal of the American Society for Mass Spectrometry* **21,** 2023–2030 (2010).

151. Kiss, A., Jungmann, J. H., Smith, D. F. & Heeren, R. M. Microscope mode secondary ion mass spectrometry imaging with a Timepix detector. *Review of Scientific Instruments* **84,** 0137041–0137047 (2013).

152. Chughtai, K. *et al.* Fiducial markers for combined 3-dimensional mass spectrometric and optical tissue imaging. *Analytical chemistry* **84,** 1817–1823 (2012).

153. Brison, J. *et al.* TOF-SIMS 3D imaging of native and non-native species within HeLa cells. *Analytical Chemistry* **85,** 10869–10877 (2013).

154. Shard, A. G. *et al.* Measuring compositions in organic depth profiling: results from a VAMAS interlaboratory study. *The Journal of Physical Chemistry B* **119,** 10784–10797 (2015).

155. Lazar, A. N. *et al.* Time-of-flight secondary ion mass spectrometry (TOF-SIMS) imaging reveals cholesterol overload in the cerebral cortex of Alzheimer disease patients. *Acta Neuropathologica* **125,** 133–144 (2013).

156. Solé-Domènech, S. *et al.* Localization of cholesterol, amyloid and glia in Alzheimer's disease transgenic mouse brain tissue using time-of-flight secondary ion mass spectrometry (ToF-SIMS) and immunofluorescence imaging. *Acta Neuropathologica* **125,** 145–157 (2013).

157. Touboul, D. *et al.* MALDI-ToF and cluster-ToF-SIMS imaging of Fabry disease biomarkers. *International Journal of Mass Spectrometry* **260,** 158–165 (2007).

158. Angerer, T. B., Magnusson, Y., Landberg, G. & Fletcher, J. S. Lipid heterogeneity resulting from fatty acid processing in the human breast cancer microenvironment identified by GCIB-ToF-SIMS imaging. *Analytical Chemistry* **88,** 11946–11954 (2016).

159. Phan, N. T., Fletcher, J. S. & Ewing, A. G. Lipid structural effects of oral administration of methylphenidate in drosophila brain by secondary ion mass spectrometry imaging. *Analytical Chemistry* **87,** 4063–4071 (2015).

160. Tian, H. *et al.* Spatiotemporal lipid profiling during early embryo development of Xenopus laevis using dynamic time-of-flight secondary ion mass spectrometry (ToF-SIMS) imaging. *Journal of Lipid Research* **55,** 1970–1980 (2014).

161. Tentschert, J. *et al.* TOF-SIMS analysis of cell membrane changes in functional impaired human macrophages upon nanosilver treatment. *Surface and Interface Analysis* **45,** 483–485 (2013).

162. Tian, H., Six, D. A., Krucker, T., Leeds, J. A. & Winograd, N. Subcellular Chemical Imaging of Antibiotics in Single Bacteria Using C60-Secondary Ion Mass Spectrometry. *Analytical Chemistry* **89,** 5050–5057 (2017).

163. Wehrli, P. M., Angerer, T. B., Farewell, A., Fletcher, J. S. & Gottfries, J. Investigating the Role of the Stringent Response in Lipid Modifications during the Stationary Phase in E. coli by Direct Analysis with Time-of-Flight-Secondary Ion Mass Spectrometry. *Analytical Chemistry* **88,** 8680–8688 (2016).

164. Hook, A. *et al.* Combinatorial discovery of polymers resistant to bacterial attachment. *Nature Biotechnology* **30,** 868–875 (2012).

165. Lee, K. *et al.* Production of advanced coronary atherosclerosis, myocardial infarction and "sudden death" in swine. *Experimental and Molecular Pathology* **15,** 170–190 (1971).

166. Wilson, R., Hartroft, W., *et al.* Pathogenesis of myocardial infarcts in rats fed a thrombogenic diet. *Archives of Pathology* **89,** 457–469 (1970).

167. Iwanaga, K. *et al.* Effects of G-CSF on cardiac remodeling after acute myocardial infarction in swine. *Biochemical and Biophysical Research Communications* **325,** 1353–1359 (2004).

168. Hood, W. B., McCarthy, B. & Lown, B. Myocardial infarction following coronary ligation in dogs: hemodynamic effects of isoproterenol and acetylstrophanthidin. *Circulation Research* **21,** 191–200 (1967).

169. Pfeffer, M. A. *et al.* Myocardial infarct size and ventricular function in rats. *Circulation Research* **44,** 503–512 (1979).

170. Mallo, M. Controlled gene activation and inactivation in the mouse. *Frontiers in Bioscience* **11,** 313–327 (2006).

171. Heine, H. L., Leong, H. S., Rossi, F. M., McManus, B. M. & Podor, T. J. *Strategies of Conditional Gene Expression in Myocardium* in *Molecular Cardiology* (2005).

172. Greene, L. A. & Tischler, A. S. Establishment of a noradrenergic clonal line of rat adrenal pheochromocytoma cells which respond to nerve growth factor. *Proceedings of the National Academy of Sciences* **73,** 2424–2428 (1976).

173. Corsetto, P. *et al.* Changes in Lipid Composition During Manganese-Induced Apoptosis in PC12 Cells. *Neurochemical Research* **41,** 258–269 (2016).

174. Denisova, N. A., Cantuti-Castelvetri, I., Hassan, W. N., Paulson, K. E. & Joseph, J. A. Role of membrane lipids in regulation of vulnerability to oxidative stress in PC12 cells: implication for aging. *Free Radical Biology and Medicine* **30,** 671–678 (2001).

175. Ikemoto, A., Kobayashi, T., Watanabe, S. & Okuyama, H. Membrane fatty acid modifications of PC12 cells by arachidonate or docosahexaenoate affect neurite outgrowth but not norepinephrine release. *Neurochemical Research* **22,** 671–678 (1997).

176. Winograd, N. & Bloom, A. *Sample Preparation for 3D SIMS Chemical Imaging of Cells* in *Mass Spectrometry Imaging of Small Molecules* (2015).

177. Breitenstein, D., Rommel, C., Stolwijk, J., Wegener, J. & Hagenhoff, B. The chemical composition of animal cells reconstructed from 2D and 3D ToF-SIMS analysis. *Applied Surface Science* **255,** 1249–1256 (2008).

178. Chandra, S. & Morrison, G. H. Sample preparation of animal tissues and cell cultures for secondary ion mass spectrometry (SIMS) microscopy. *Biology of the Cell* **74,** 31–42 (1992).

179. Malm, J., Giannaras, D., Riehle, M. O., Gadegaard, N. & Sj vall, P. Fixation and drying protocols for the preparation of cell samples for time-of-flight secondary ion mass spectrometry analysis. *Analytical Chemistry* **81,** 7197–7205 (2009).

180. Phan, N. T., Fletcher, J. S., Sjövall, P. & Ewing, A. G. ToF-SIMS imaging of lipids and lipid related compounds in Drosophila brain. *Surface and Interface Analysis* **46,** 123–126 (2014).

181. Bich, C. *et al.* Argon cluster ion source evaluation on lipid standards and rat brain tissue samples. *Analytical Chemistry* **85,** 7745–7752 (2013).

182. Sjövall, P., Johansson, B. & Lausmaa, J. Localization of lipids in freeze-dried mouse brain sections by imaging TOF-SIMS. *Applied Surface Science* **252,** 6966–6974 (2006).

183. Sämfors, S., Ståhlman, M., Klevstig, M., Borén, J. & Fletcher, J. S. Localised lipid accumulation detected in infarcted mouse heart tissue using ToF-SIMS. *International Journal of Mass Spectrometry* (2017).

184. Angerer, T. B., Mohammadi, A. S. & Fletcher, J. S. Optimizing sample preparation for anatomical determination in the hippocampus of rodent brain by ToF-SIMS analysis. *Biointerphases* **11,** 02A3191–10 (2016).

185. Piwowar, A. M. *et al.* C60-ToF SIMS imaging of frozen hydrated HeLa cells. *Surface and Interface Analysis* **45,** 302–304 (2013).

186. Fletcher, J. S., Rabbani, S., Henderson, A., Lockyer, N. P. & Vickerman, J. C. Three-dimensional mass spectral imaging of HeLa-M cells–sample preparation, data interpretation and visualisation. *Rapid Communications in Mass Spectrometry* **25,** 925–932 (2011).

187. Colliver, T. L. *et al.* Atomic and molecular imaging at the single-cell level with TOF-SIMS. *Analytical Chemistry* **69,** 2225–2231 (1997).

188. Roddy, T. P., Cannon, D. M., Ostrowski, S. G., Ewing, A. G. & Winograd, N. Proton transfer in time-of-flight secondary ion mass spectrometry studies of frozen-hydrated dipalmitoylphosphatidylcholine. *Analytical Chemistry* **75,** 4087–4094 (2003).

189. Carado, A. *et al.* C60 secondary ion mass spectrometry with a hybrid-quadrupole orthogonal time-of-flight mass spectrometer. *Analytical Chemistry* **80,** 7921–7929 (2008).

190. Smith, D. F. *et al.* High mass accuracy and high mass resolving power FT-ICR secondary ion mass spectrometry for biological tissue imaging. *Analytical and Bioanalytical Chemistry* **405,** 6069–6076 (2013).

191. Passarelli, M. K. *et al.* The 3D OrbiSIMS label-free metabolic imaging with subcellular lateral resolution and high mass-resolving power. *Nature Methods* **14,** 1175–1183 (2017).

192. Hill, R., Blenkinsopp, P., Thompson, S., Vickerman, J. & Fletcher, J. S. A new time-of-flight SIMS instrument for 3D imaging and analysis. *Surface and Interface Analysis* **43,** 506–509 (2011).

193. Fletcher, J. S. *et al.* A new dynamic in mass spectral imaging of single biological cells. *Analytical chemistry* **80,** 9058–9064 (2008).

194. Willse, A. & Tyler, B. Poisson and multinomial mixture models for multivariate SIMS image segmentation. *Analytical Chemistry* **74,** 6314–6322 (2002).

195. Nygren, H. & Malmberg, P. Silver deposition on freeze-dried cells allows subcellular localization of cholesterol with imaging TOF-SIMS. *Journal of Microscopy* **215,** 156–161 (2004).

196. Smentkowski, V., Keenan, M., Ohlhausen, J. & Kotula, P. Multivariate statistical analysis of concatenated time-of-flight secondary ion mass spectrometry spectral images. Complete description of the sample with one analysis. *Analytical Chemistry* **77,** 1530–1536 (2005).

197. Tyler, B. J., Rayal, G. & Castner, D. G. Multivariate analysis strategies for processing ToF-SIMS images of biomaterials. *Biomaterials* **28,** 2412–2423 (2007).

198. Henderson, A., Fletcher, J. S. & Vickerman, J. C. A comparison of PCA and MAF for ToF-SIMS image interpretation. *Surface and Interface Analysis* **41,** 666–674 (2009).

199. Hanrieder, J., Malmberg, P., Lindberg, O. R., Fletcher, J. S. & Ewing, A. G. Time-of-flight secondary ion mass spectrometry based molecular histology of human spinal cord tissue and motor neurons. *Analytical Chemistry* **85,** 8741–8748 (2013).

200. Wall, R., Ross, R. P., Fitzgerald, G. F. & Stanton, C. Fatty acids from fish: the anti-inflammatory potential of long-chain omega-3 fatty acids. *Nutrition Reviews* **68,** 280–289 (2010).